

UNCLASSIFIED

AD 294 395

*Reproduced
by the*

ARMED SERVICES TECHNICAL INFORMATION AGENCY
ARLINGTON HALL STATION
ARLINGTON 12, VIRGINIA



UNCLASSIFIED

N-63-2-34

**THERMOLUMINESCENCE AND ELECTRON PARAMAGNETIC
RESONANCE OF AMINO ACIDS, POLYPEPTIDES AND PROTEINS
IRRADIATED WITH ULTRAVIOLET LIGHT**

By
J. Gill and M. Weissbluth

Technical Report No. 2
Prepared under Office of Naval Research Contract
Nonr-225(36) (NR 304-492)

B. L. Report No. 77
October 1962

Reproduction in whole or part is permitted for
any purpose of the United States Government



Biophysics Laboratory
W. W. HANSEN LABORATORIES OF PHYSICS
STANFORD UNIVERSITY
STANFORD, CALIFORNIA

294 395

NOTICE: When government or other drawings, specifications or other data are used for any purpose other than in connection with a definitely related government procurement operation, the U. S. Government thereby incurs no responsibility, nor any obligation whatsoever; and the fact that the Government may have formulated, furnished, or in any way supplied the said drawings, specifications, or other data is not to be regarded by implication or otherwise as in any manner licensing the holder or any other person or corporation, or conveying any rights or permission to manufacture, use or sell any patented invention that may in any way be related thereto.

BIOPHYSICS LABORATORY
W. W. Hansen Laboratories of Physics
Stanford University
Stanford, California

THERMOLUMINESCENCE AND ELECTRON PARAMAGNETIC RESONANCE OF
AMINO ACIDS, POLYPEPTIDES AND PROTEINS IRRADIATED WITH ULTRAVIOLET LIGHT

By

J. Gill and M. Weissbluth

TECHNICAL REPORT No. 2

October 1962

Prepared under Office of Naval Research
Contract Nonr-225(36) (NR 304-492)

B. L. Report No. 77

Foreword

The main body of the present report is based on a dissertation by J. Gill, submitted to the Physics Department of Stanford University in partial fulfillment of the requirements for the Ph.D. degree. Portions of this work have been reported at meetings of The Biophysical Society, February 1962, Washington, D. C. and of The American Physical Society, August 1962, Seattle, Washington.

TABLE OF CONTENTS

	Page
I Introduction and survey	1
II Theory and kinetics of thermoluminescence	14
III Results and interpretation of thermoluminescence experiments	45
IV Results and interpretation of electron paramagnetic resonance experiments	75
Summary	91
Appendices:	
I Outline of calculation of probability for thermal excitation of trapped charge	93
II Computer program for glow curves	96

LIST OF FIGURES

	Page
1. (a) A single polypeptide chain. (b) Polypeptides arranged in a pleated sheet configuration	3
2. The α -helix	4
3. Schematic representation of two mechanisms of charge transfer along a chain of fixed molecules	6
4. Energy level diagram indicating valence and conduction bands of states plus the relatively few states or traps in the energy gap	16
5. Energy level diagram indicating the two thin shells of states, one in the energy gaps, one in the conduction band	18
6. Energy of singlet (S) and triplet (T) state orbitals as a function of the angle of twist about the axis of the ethylenic double bond	26
7. The relationship between heating rate and peak temperature	30
8. Block representation of a polypeptide	32
9. Block representation of a polypeptide showing the ordering of trapping sites used in the Markov analysis of charge migration	32
10. Cross section of the thermoluminescence cryostat	46
11. Top view of the thermoluminescence cryostat showing the inlet for the dry nitrogen gas, the thermocouple lead and the ac cord to the heater	46
12. A block diagram of the thermoluminescence apparatus	47
13. Side view of the cryostat in position under the black box containing the photomultiplier tube	48
14. The thermoluminescence apparatus as described in the text with the cryostat in position beneath the ultraviolet lamp	49
15. Typical glow curve of uv irradiated L-tyrosine	51
16. Semilogarithmic plot of intensity versus $100/T$ for the initial part of the tyrosine glow curve	53

	Page
17. Typical glow curve of uv irradiated L-phenylalanine	54
18. Semilogarithmic plot of the phosphorescence decay from uv irradiated L-phenylalanine at 77° K	60
19. Semilogarithmic plot of intensity versus 100/T for the initial part of the phenylalanine glow curve	61
20. A comparison of experimental points and theoretical curves computed using the parameters listed	62
21. A comparison of experimental points from an L-tyrosine glow curve with theoretical glow curves computed using the parameters listed	64
22. Glow curve of uv irradiated poly L-phenylalanine	69
23. Glow curve of uv irradiated trypsin	72
24. Semilogarithmic plot of the decay of phosphorescence from uv irradiated egg albumin at 77° K	73
25. Comparison of theoretical glow curves from a monomer and a four-unit polymer	74
26. First derivative traces of paramagnetic resonance absorption in glycylglycine and glycine measured as a function of magnetic field H	79
27. First derivative traces of paramagnetic resonance absorption in L-cystine and L-cysteine	82
28. First derivative traces of paramagnetic resonance absorption in reduced glutathione	84
29. First derivative trace of paramagnetic resonance absorption developed in polycrystalline trypsin after uv irradiation at 77° K	85
30. First derivative traces of paramagnetic resonance absorption developed in egg albumin after uv irradiation at 77° K	86
31. First derivative trace of paramagnetic resonance absorption developed in bovine hemoglobin after uv irradiation at 77° K	89

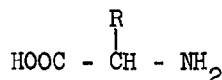
CHAPTER I

INTRODUCTION AND SURVEY

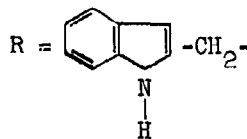
The research which is the subject of this thesis consists of (1) the development of theories and kinetic expressions for thermoluminescence from macroscopic crystals, molecular crystals and amorphous solids, (2) the measurement of thermoluminescence from amino acids, polypeptides and proteins which had been subjected to ultraviolet irradiation, (3) the measurement of electron paramagnetic resonance developed in these materials as a result of ultraviolet irradiation.

Proteins, polypeptides and their basic subunits, amino acids, are ubiquitous and essential constituents of all biological systems. The polymers serve as structural units, as catalysts of biochemical reactions, as hormones and as other functional units. Proteins and polypeptides are composed of one or a few chains of mixed polymers in which the various amino acid molecules are joined together with peptide bonds.¹ The chains in turn are held together with covalent or hydrogen bonds and possibly by van der Waals forces.^{1,2}

The generalized structural formula of amino acids is shown below.



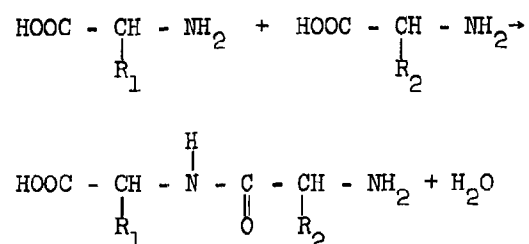
R stands for residue or side group. There are about twenty different side groups found in naturally occurring amino acids. They range from R = H in glycine to



¹J. L. Oncley, Rev. Mod. Phys. 31, 30 (1959).

²A. Rich, Rev. Mod. Phys. 31, 50 (1959).

in tryptophan. Polymerization of amino acids takes place with the splitting out of H_2O . The reaction is

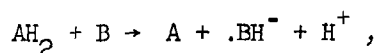


and may be repeated at either end of the molecule. R_1 and R_2 may be any of the twenty side groups.

On the basis of x-ray diffraction and other studies by many workers, it is now believed that the polypeptides may assume three different configurations. These are: (1) the extended zig-zag or pleated-sheet configuration shown in Fig. 1, (2) the α -helix configurations² shown in Fig. 2 and (3) the random coil. The pleated-sheet configuration is found in structural or filamentous protein. The α -helix and the random coil configurations are both found in many globular and catalytic proteins.

Enzymes, i.e., catalytic proteins, are able to promote a wide variety of biochemical reactions without being used up in the process. Of particular interest from the point of view of the physics involved are the charge-transfer reactions.

Such reactions may be separated into two groups according to whether they are ordinary collision mediated reactions or not. A collision mediated reaction is one in which two molecules moving about in solution collide and form an excited complex. This complex then breaks apart into molecules different from the initial reactants. A common example is



where A and B are molecules whose exact structures are of no concern here.

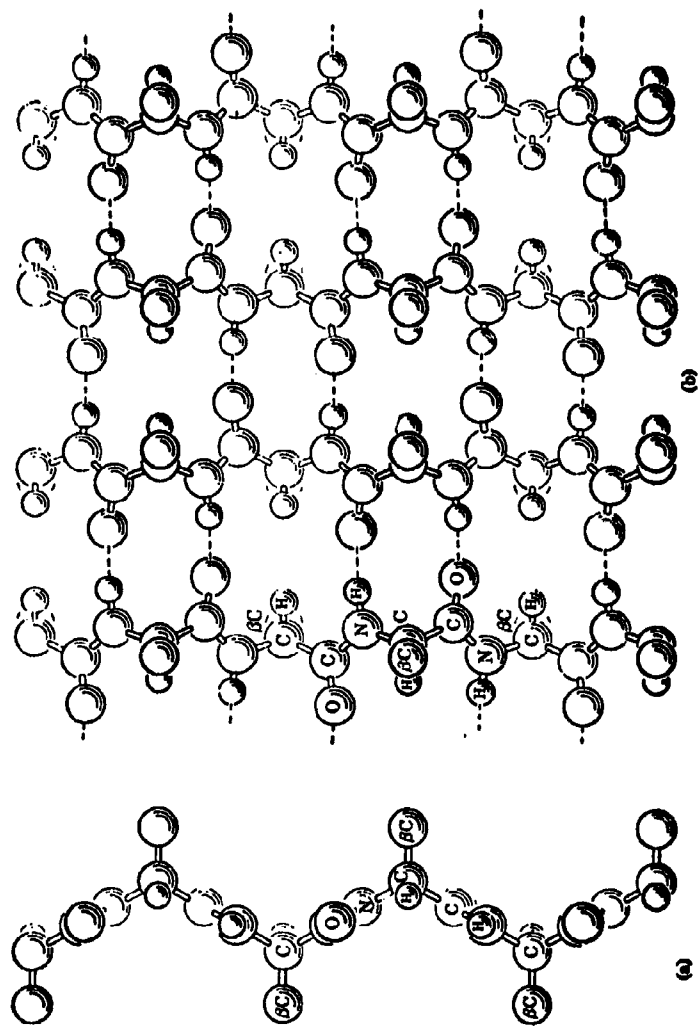


FIG. 1--(a) A single polypeptide chain, (b) Polypeptides arranged in a pleated sheet configuration [from R. E. Marsh, R. B. Corey, and L. Pauling, *Biochim. et Biophys. Acta* 16, 1 (1955)].

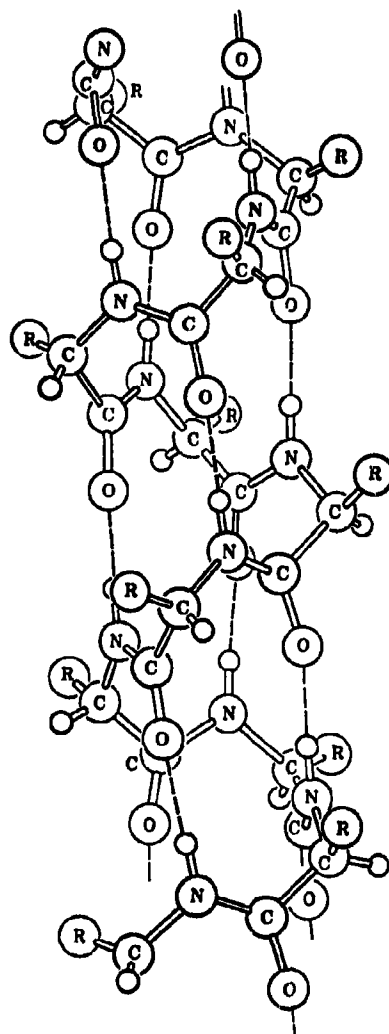


FIG. 2--The α -helix [from R. B. Corey and L. Pauling, Rend. ist. lombardo sci. 89, 10 (1955)].

In charge transfer reactions which are not collision mediated, the charge transfer may take place across distances of from 10 to 50 Angstroms or more. Such reactions are best discussed in terms of examples, even though the reaction mechanisms for these examples are not completely understood.

The biological electron transport system consists of oxidation-reduction enzymes which are located in the membrane of the mitochondria. Electrons move through this sequence of enzymes driving the formation of energy-rich compounds. The enzymes pass the electron to one another apparently without the use of intermediate shuttle molecules.³ Furthermore, the enzymes are restricted to certain sites in or on the membrane. They may or may not have complete freedom of rotation at these sites.

Chance⁴ has proposed two mechanisms for charge transfer among these enzymes. In one mechanism, freedom of rotation of the molecules is postulated to permit collision mediated charge exchanges between the prosthetic groups of neighboring enzymes. In the other mechanism, the molecules are assumed to be fixed, and the charges move through them. These two mechanisms are schematically indicated in Fig. 3. In these diagrams, the circles represent the protein part, the straight line the prosthetic group of the enzyme. Arrows in the upper diagram indicate the notion that the enzymes rotate until the prosthetic groups of two neighboring enzymes are touching, whereupon charge transfer takes place from one group to the other. In the lower diagram, the arrows indicate a hypothetical migration of charge through the protein from one prosthetic group to the next. These diagrams are a great oversimplification in that

³A. L. Lehninger, Rev. Mod. Phys. 31, 136 (1959).

⁴B. Chance and G. R. Williams, Advances in Enzymol. 17, 65 (1959).

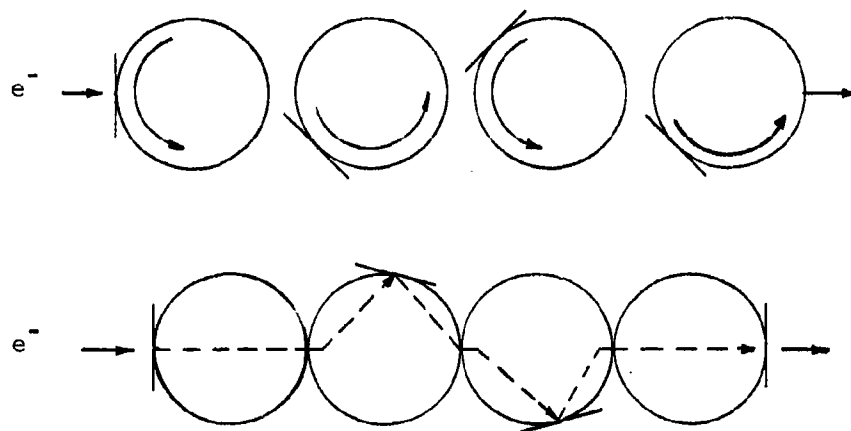


FIG. 3--Schematic representation of two mechanisms of charge transfer along a chain of fixed molecules (adapted from Chance and Williams⁴).

they leave out the chemistry known to be associated with the electron transfer. Information and references on this chemistry may be found in Lehninger's article.³ Though neither of these mechanisms has been substantiated, the second does serve as an example of a charge transfer which takes place without a collision of two molecules.

A second example is also the work of Chance.⁵ He has studied a light-induced intermolecular oxidation-reduction reaction between bacterial chlorophyll and a cytochrome, and has found that this reaction still proceeds at temperatures as low as 80° K. Spectroscopic data show that in this reaction, the cytochrome is oxidized from the ferrous to the ferric state. The quantum requirement for this reaction is two photons per transferred charge. The photons are absorbed by chlorophyll molecules. Since only three percent of the chlorophyll molecules are contiguous with cytochrome molecules, it follows that the energy produced when any chlorophyll molecule absorbs a photon can effect the oxidation over a distance large compared to the size of the molecule. And since the reaction proceeds at 80° K, a bimolecular collision is clearly not involved. Several explanations are possible as to how the oxidation takes place.

- (1) The photon excites an electron in the chlorophyll and it or its vacancy migrates to the site of a cytochrome where oxidation takes place.
- (2) The excitation caused by the photon migrates as an exciton to the cytochrome and there promotes the oxidation.
- (3) The photon may initiate a proton migration⁶ which culminates in the oxidation. An inductive resonance between an excited chlorophyll and a cytochrome is unlikely because the emission spectrum of chlorophyll and the absorption spectrum

⁵B. Chance and M. Nishimura, Proc. Natl. Acad. Sci. U.S. 46, 19 (1960).

⁶A. Terenin, E. Putzeiko, I. Akimov, Discussions Faraday Soc. 27, 83 (1959).

of cytochrome do not overlap.⁷ However, there are no data at present which indicate which of the three explanations given above is closest to the truth.

Much work has gone into the charge and energy transfer problem and into investigations of the semiconductor properties of proteins.^{8,9,10} It has been found possible to calculate the width and separation of valence and conduction bands for certain configurations of proteins.⁹ Experiments on a number of proteins in the polycrystalline or dry gel form have shown that the electrical conductivity is proportional to $\exp(-\Delta E/kT)$ where ΔE is an activation energy of 2.6 to 3.1 ev.¹⁰ However, it is not clear whether the band model of semiconductivity is valid for systems such as protein or amino acid molecular crystals. Nor is it clear that this model is pertinent to charge transport within protein molecules. One can argue against the suitability of the band model for proteins and amino acid crystals in the following way. Molecules such as amino acids, proteins and the like do not form ionic or covalent crystals but rather amorphous solids or crystals in which the molecules are held to one another by weak forces such as the van der Waals force. There is but slight interpenetration of molecular charge clouds at the van der Waals radius. As a result, any intermolecular conduction band capable of supporting charge transfer between molecules will be very narrow. Even when the molecules are linked by hydrogen bonds,¹¹ where the electron

⁷Th. Förster, Discussions Faraday Soc. 27, 7 (1959).

⁸A. Szent-Györgyi, Nature 148, 157 (1941).

⁹M. G. Evans and J. Gergely, Biochim. Biophys. Acta 3, 188 (1949).

¹⁰D. Eley and D. Spivey, Trans. Faraday Soc. 56, 1432 (1960).

¹¹L. Orgel, Rev. Mod. Phys. 31, 100 (1959).

overlap is enhanced by the presence of the intermediate proton, the interaction, hence the band width, is very small.

The velocity of an electron in a conduction band is the group velocity of a wave packet, which is $(1/\hbar)(\partial E_k/\partial k)$, where E_k is the energy as a function of the wave vector k . Since the range of k in each band is $2\pi/a$ (a = lattice parameter) the narrower the band, the smaller is the average value of $\partial E_k/\partial k$ and the smaller is the velocity. In order for an electron to "see" the periodicity of the lattice, it must traverse several unit cells between phonon collisions. If the electron velocity is so low that this does not happen, the Bloch functions are no longer good zero-order approximations for the electron-wave functions and ordinary conductivity, i.e., band theory is inappropriate. In this case it seems better to invert the usual orders of approximation, treating the electron-phonon interaction in zero order to get a self-trapped charge and then introducing the periodic potential of the crystal or molecule as a perturbation which gives rise to a random walk migration of the trapped charge.

In a recent review article¹² Garrett points out that the observed temperature dependence of conductivity in organic crystals may be inherent in the charge mobility, instead of the number of charge carriers. The random walk migration of trapped charges does give rise to a temperature dependence of mobility of the form $\exp(-\Delta E/kT)$ where ΔE is a thermal activation energy. Garrett also mentions that no Hall effect has been observed in organic semiconductors (as of 1959) and that Seebeck effect investigations indicate the charge carriers are positive.

¹²C.G.B. Garrett in Semiconductors (edited by N. B. Hannay, Reinhold, New York, 1959).

Ioffe¹³ has suggested that the observed conductivity in organic solids can be described in terms of the mobility of ions in solid electrolytes. Such a description gives rise to the observed temperature dependence.

Charge conduction within a polymer molecule such as the α -helix polypeptide (see Fig. 2), if it occurs, is probably confined either to the polymer back bone or to the hydrogen bond system. In either case the conducting charge must follow a crooked path, being scattered into a new direction after traveling only a few Angstroms. The momentum vector k is not a good quantum number for charges suffering such scattering. Their behavior is best described by localized wave functions which migrate along the polymer. Thus the band model also seems inappropriate for the description of intramolecular charge transport in proteins.

Additional information and references on charge and energy migration in biological systems may be found in volume 27 of the Discussions of the Faraday Society.

It has been known for sometime that irradiation with ultraviolet light causes electronic excitations in biological molecules. The events which take place in these molecules subsequent to irradiation often involve energy or charge transfer. When the ultraviolet irradiation is performed at low temperature, such as 77° K, these events are slowed or modified and may be observed experimentally. Thus observations such as the thermoluminescence and electron paramagnetic resonance experiments reported in this thesis shed some light on charge and energy migration processes.

¹³A. F. Ioffe, Physics of Semiconductors (Infosearch, London, 1960).

Thermoluminescence is the name given to visible and ultraviolet light released from a substance as a result of heating. This phenomenon has been known for about 300 years. Vincenzo Cascariolo, a cobbler in Bologna, may have observed it as early as 1602.¹⁴ Cascariolo, an alchemist by avocation, found some particularly interesting rocks which sparkled in the sunlight and proceeded to heat them in his furnace. In doing so, he apparently observed the thermal release of phosphorescence instead of the formation of precious metals as he had hoped. There are reliable reports that Robert Boyle observed thermoluminescence from heated diamonds in 1663. And in 1681, the Berlin physician Johann Elsholtz published an account of experiments in which fluorspar powder was formed into various symbols on a metal plate, then heated and made to glow.

These investigators noticed that the substances did not glow when cooled and reheated. They realized that heating released light from the substance but that heat was not transformed into light.

For sometime it was believed that the heating of thermoluminescent materials released trapped sunlight. However, it eventually became well known that the color of the luminescence was a characteristic of the material and that no luminescence appeared unless the wavelength of the exciting light was somewhat shorter than the characteristic luminescence wavelength for that material. Toward the end of the 18th Century it was reported that various materials would exhibit thermoluminescence after exposure to cathode, radium and other rays as well as to visible light. This information gave rise to the idea, essentially correct, that the radiation produced some kind of change or excitation in the material,

¹⁴R. W. Wood, "Fluorescence and Phosphorescence" in Encyclopedia Britannica.

that heating permitted the material to relax or change back to the normal state and that light was given off during this relaxation.

In this century, the modern band theories of solids have permitted a quantitative understanding of thermoluminescence from inorganic solids, particularly as a result of the experimental work of Urbach and his collaborators¹⁵ in 1930 and by Randall and Wilkins¹⁶ during the early 1940's. This work has been summarized in some detail by Wood¹⁴ and by Garlick.¹⁷

The study of thermoluminescence from organic or biological systems appears to have a much shorter history. Arnold and Sherwood observed thermoluminescence from chloroplasts which had been irradiated with white light at room temperature.¹⁸ Chloroplasts are subcellular bodies which contain chlorophyll, cytochromes and a number of enzymes important for photosynthesis. Arnold and Sherwood thus demonstrated that chloroplasts could store energy received in the form of visible light.

Augenstine and co-workers^{19,20} studied thermoluminescence from amino acids and proteins in an attempt to understand the effects of x-ray irradiation on these compounds. They cooled powdered crystalline samples to liquid nitrogen temperature and irradiated them with Cobalt-60 gamma

¹⁵F. Urbach, et al., Sitzung Berichte, Vienna Academy of Science (1930).

¹⁶J. T. Randall and M. H. Wilkins, Proc. Roy. Soc. A 184, 366 (1945).

¹⁷C.F.J. Garlick, "Luminescence" in Encyclopedia of Physics (edited by S. Flügge, Volume XXVI, 1-128, 1958).

¹⁸W. Arnold and H. K. Sherwood, Proc. Natl. Acad. Sci. 43, 105 (1957); J. Phys. Chem. 63, 7 (1959).

¹⁹L. G. Augenstine, J. G. Carter, D. R. Nelson and H. P. Yockey, Radiation Research Supplement 2, 19 (1960).

²⁰C. J. Weinberg, D. R. Nelson, J. G. Carter and L. G. Augenstine, J. Chem. Phys. 36, 2869 (1962).

rays. After irradiation, the samples were heated at a linear rate and the thermoluminescence intensity as a function of time or temperature was measured. This function is known as the glow curve.

Augenstine et al., have obtained the following results. (1) For amino acids containing ring structures thermal activation energies for the various peaks in the glow curve are near 0.2 ev while for proteins, values are less than 0.1 ev. (2) Thermoluminescence intensity from amino acids which contain ring structure is as much as three orders of magnitude greater than that from nonring amino acids. (3) In amino acid crystals, the chemical structure is more closely correlated with the characteristics of the thermoluminescence than is the intermolecular arrangement as reflected in such a parameter as the crystal space group.

The thermoluminescence work reported in this thesis had two goals: (1) a theory of thermoluminescence applicable to the materials studied, and (2) knowledge of the behavior of the ultraviolet excited charge from a study of the glow-curve kinetics. A development of kinetics and a discussion of possible mechanisms for thermoluminescence are contained in Chapter II. Results of the thermoluminescence experiments are presented in Chapter III. Chapter IV contains a sketch of the theory of electron paramagnetic resonance together with the results of the experiments.

CHAPTER II

THEORY AND KINETICS OF THERMOLUMINESCENCE

In this chapter three theoretical expressions for thermoluminescence intensity will be developed. The distinguishing characteristic of each of these developments is the choice of the physical model of the luminescent material on which the development is based. The model usually used^{1,2} and the one to be described first is the crystal model, involving valence and conduction bands, plus various electron and hole trapping sites. Next to be developed is a simple molecular model in which each molecule absorbs, stores and emits energy independently of its environment. This model proves useful in interpreting thermoluminescence of aromatic amino acids. The third model is a polymer or one-dimensional crystal model in which trapped charges may hop from one monomer or unit cell to an adjacent one. This third point of view is proposed to describe thermoluminescence from polypeptides and proteins. In each case, the nature of the energy trapping or metastable excited state is discussed but not specified precisely and the form of the temperature-dependent probability for thermal depopulation of these states is assumed. It is also assumed that radiative decay to the ground state follows thermal emptying of a metastable excited state with 10^{-4} sec. The kinetics of the luminescence is then derived on the basis of the model and these initial assumptions.

A theory of thermoluminescence from crystalline materials is given by Augenstein, et al.³ They present data on the x-ray-induced glow curves

¹See for example, D. Curie, Luminescence Cristalline (Dunod, Paris, 1960).

²G.F.J. Garlick, "Luminescence" in Encyclopedia of Physics (edited by S. Flügge, Volume XXVI, 1-128, 1958).

³L. G. Augenstein, J. G. Carter, D. R. Nelson, and H. P. Yockey, Radiation Research Supplement 2, 19 (1960).

of proteins and amino acids interpreted in terms of their theory. We wish to give a more detailed theory, based to some extent on the work of Halperin and Braner.⁴ Their notation will be used here.

To begin with, we assume that our sample is a crystalline material in which the electrons are subjected to a periodic potential so that the Bloch functions are appropriate as electron-wave functions and the energy levels of the electrons separate into bands. Also, we suppose that there is a gap between the top of the highest band of filled states, the valence band, and the lowest band of empty states, the conduction band. We assume that the width of this gap is much greater than kT at room temperature. Because of the existence of lattice imperfections, randomly distributed dipoles, etc., there will be localized states available to the electrons and holes within the energy gap. The energy E is measured from any convenient level, such as the top of the valence band. The magnitude of the energy gap will then be E_g , as shown in Fig. 4.

After ultraviolet or x-ray irradiation, a number of electrons will have been excited into the conduction band and subsequently trapped in the localized electron states, called traps from now on. The holes left behind in the valence band will have migrated to the localized hole states, called luminescence centers. There are, say, $n_t(E)dE$ trapped electrons per unit volume at energy E to $E + dE$, $m(E')dE'$ holes per unit volume at energy E' to dE' . As the sample is heated, the trapped electrons and/or holes acquire sufficient thermal energy to escape into the conduction or valence band. Once excited into bands, the charges migrate, and the electrons and holes recombine. In describing this process,

⁴A. Halperin and A. A. Braner, Phys. Rev. 117, 408 (1960).

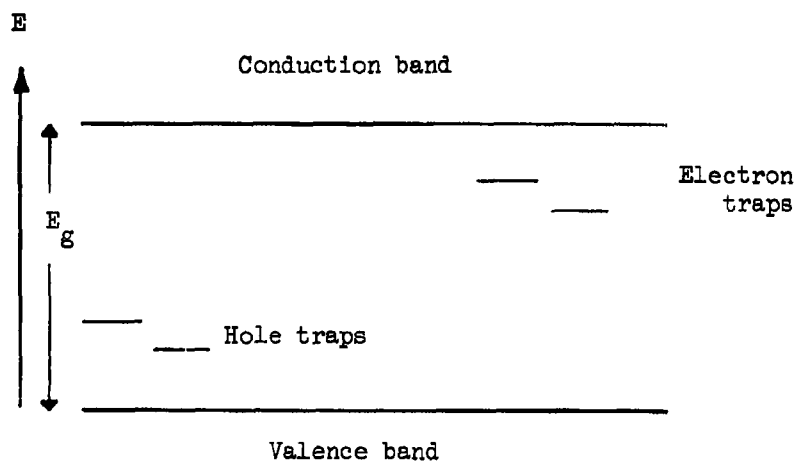


FIG. 4--Energy level diagram indicating valence and conduction bands of states plus the relatively few states or traps in the energy gap.

we assume that the electrons are the thermally activated particles, the holes remaining trapped. The kinetics are the same if the roles are reversed.

Before deriving these kinetics, we consider the equilibrium distribution of electrons in the crystal. Let $N(E)$ be the density of electron states throughout the valence band, conduction band, and energy gap. Let $f(E)$ stand for the Fermi-Dirac distribution

$$f(E) = \frac{1}{\exp[(E - E_F)/kT] + 1} , \quad (2-1)$$

in which E_F is the Fermi energy.

Let $n(E) = N(E)f(E)$ stand for the equilibrium distribution of electrons in the crystal. Next, assume the energy E_F is located within the energy gap sufficiently far from any trapping levels so that, to a good approximation,

$$f(E) = \exp\left(-\frac{E - E_F}{kT}\right) \quad (2-2)$$

$$n(E) = N(E)\exp\left(-\frac{E - E_F}{kT}\right) . \quad (2-3)$$

Consider two thin constant energy shells of electron states, one about E_t in the energy gap and the other at E_c near the bottom of the conduction band as shown in Fig. 5. The equilibrium electron densities in these two shells are

$$\left. \begin{aligned} n(E_t) &= N(E_t) \exp\left(-\frac{E_t - E_F}{kT}\right) \\ n(E_c) &= N(E_c) \exp\left(-\frac{E_c - E_F}{kT}\right) \end{aligned} \right\} . \quad (2-4)$$

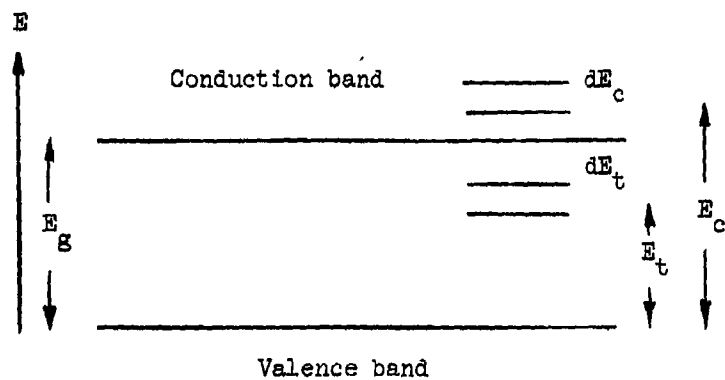


FIG. 5--Energy level diagram indicating the two thin shells of states, one in the energy gaps, one in the conduction band, as described in the text.

$N(E_t) - n(E_t)$ = number per unit volume of unoccupied trap states in the interval E_t to $E_t + dE_t$.

$N(E_c) - n(E_c)$ = number per unit volume of unoccupied conduction states in the interval E_c to $E_c + dE_c$.

The principles of detailed balance tells us that at equilibrium the number of electrons excited from the shell at E_t to the shell at E_c per unit time is equal to the number trapped from E_c to E_t per unit time. This fact can be used to find the temperature dependence of the rate of excitation of electrons from E_t to E_c . Let

$$\gamma_1(T)[N(E_c) - n(E_c)]$$

be the probability per unit time that an electron in a trap at E_t will be excited to the conduction band at E_c . Let

$$\gamma_2[N(E_t) - n(E_t)]$$

be the probability per unit time that an electron in the conduction band will fall into one of the $[N(E_t) - n(E_t)]$ empty traps available in a unit volume. We assume γ_2 is not dependent on temperature. The parameters $\gamma_1(T)$, γ_2 contain such quantities as the matrix element for the transition involved and the energy distribution of phonons which are involved in the transition. Attempts at a calculation of these quantities have been made by several authors.^{5,6}

From the statement that the number of electrons excited per unit time equals the number trapped we get the equation

$$n(E_t)\gamma_1(T)[N(E_c) - n(E_c)] = n(E_c)\gamma_2[N(E_t) - n(E_t)] . \quad (2-5)$$

⁵R. Kubo, Phys. Rev. 86, 929 (1952).

⁶B. Goodman, A. W. Lawson, L. I. Schiff, Phys. Rev. 71, 174 (1947).

Using Eq. (2-4) and cancelling like factors from both sides we can rewrite Eq. (2-5) as

$$\gamma_1(T) \left[1 - \exp\left(-\frac{E_c - E_F}{kT}\right) \right] \exp\left(-\frac{E_t}{kT}\right) = \gamma_2 \left[1 - \exp\left(-\frac{E_t - E_F}{kT}\right) \right] \exp\left(-\frac{E_c}{kT}\right)$$

or, consistent with approximation (2-2), as

$$\gamma_1(T) = \gamma_2 \exp\left(-\frac{E_c - E_t}{kT}\right) .$$

On the basis of this result we will take

$$\left. \begin{aligned} \gamma_2 &= \text{constant} = \gamma \\ \gamma_1(T) &= \gamma \exp\left(-\frac{E_c - E_t}{kT}\right) \end{aligned} \right\} \quad (2-6)$$

and assume these results are valid for any distribution of electrons in the crystal. In the appendix we outline a calculation of $\gamma_1(T)$ due to Kubo.⁵ Using the Einstein model of a crystal and certain additional assumptions, he obtains the same functional form of $\gamma_1(T)$ as (2-26) and an expression for γ .

The simplest glow curve has one peak and all of the emitted photons have the same energy. Such a curve can be described on the basis of one trapping level at energy E_t , N_t traps per unit volume, and one level of trapped holes. At the end of the irradiation period, let us say there are n_t trapped electrons per unit volume. Since the probability for thermal excitation of a trapped electron to energy E' within the conduction band is proportional to

$$\exp\left(-\frac{E' - E_t}{kT}\right) ,$$

nearly all thermally excited electrons will go to states near the bottom of the conduction band where $E' = E_c$.

It is helpful to modify notation at this point to discuss changes in electron and hole concentration with time. Let $n_c = n(E_c)$, $N_c = N(E_c)$, $n_t = n(E_t)$, $N_t = N(E_t)$. In what follows, t refers to traps when it appears as a subscript and to time when it appears as the argument of a function. Thus $n_t(t)$ is the density of electrons in traps at energy E_t at time t . In this notation, the change in the concentration of trapped electrons during time dt is

$$dn_t = -n_t \gamma (N_c - n_c) \exp\left(-\frac{E_c - E_t}{kT}\right) dt + n_c \gamma (N_t - n_t) dt. \quad (2-7)$$

The change in the concentration of conduction electrons during this interval is

$$dn_c = -dn_t - n_c A m dt,$$

where A is a constant depending on the recombination efficiency and $m(t)$ is the number of holes per unit volume. The change in the concentration of holes during this interval is

$$dm = -n_c A m dt.$$

The set of differential equations describing the kinetics of return to equilibrium distribution is

$$\frac{dn_t}{dt} = -n_t \gamma (N_c - n_c) \exp\left(-\frac{E_c - E_t}{kT}\right) + n_c \gamma (N_t - n_t) \quad (2-8)$$

$$\frac{dn_c}{dt} = -\frac{dn_t}{dt} + \frac{dm}{dt} \quad (2-9)$$

$$\frac{dm}{dt} = -mA n_t. \quad (2-10)$$

Braner and Halperin⁴ give a careful discussion of the solution to (2-8), (2-9) and (2-10) using the approximation $dn_c/dt = 0$.

P. K. Weyl⁷ derives kinetics for thermoluminescence using a different approximation. He replaces $n_c(t)$ with what he calls the thermodynamic equilibrium value

$$n_t(t) \exp\left(-\frac{E_c - E_t}{kT}\right).$$

This replacement is incorrect since it does not take into account the difference in the density of states between the energy gap and the conduction band.

The approximation we have developed begins by assuming first that the states of the conduction band are always largely unoccupied, second that were it not for recombination of conduction band electrons with holes, n_c and n_t would be in approximate thermal equilibrium. The relative rates of recombination and retrapping depend upon the ratio A/γ . The greater this ratio, the more will n_c be reduced from its equilibrium value with respect to n_t .

On the basis of this reasoning we put

$$n_c(t) = \exp\left(-\frac{A}{\gamma}\right)\left(\frac{N_c}{N_t}\right) n_t \exp\left(-\frac{E_c - E_t}{kT}\right) \quad (2-11)$$

in the second term on the right-hand side of Eq. (2-8). These two approximations change (2-8) to

$$\begin{aligned} \frac{dn_t}{dt} = & -n_t \gamma N_c \exp\left(-\frac{E}{kT}\right) \left[1 - \exp\left(-\frac{A}{\gamma}\right)\right] \\ & + n_t^2 \frac{\gamma N_c}{N_t} \exp\left(-\frac{A}{\gamma}\right) \exp\left(-\frac{E}{kT}\right) \end{aligned} \quad (2-12)$$

where $E = E_c - E_t$ from now on. This equation is of the form known as

⁷P. K. Weyl, J. Chem. Phys. 26, 547 (1957).

Bernoulli's equation. The solution is

$$n_t(t) = \frac{n_t(0) \exp[-\int_0^t B(t') dt']}{1 - n_t(0) \int_0^t C(t') \exp[-\int_0^{t'} B(t'') dt''] dt'} \quad (2-13)$$

$$B(t) = \gamma N_c \left[1 - \exp\left(-\frac{A}{\gamma}\right) \right] \exp\left[-\frac{E}{kT(t)}\right] \quad (2-14)$$

$$C(t) = \frac{\gamma N_c}{N_t} \exp\left(-\frac{A}{\gamma}\right) \exp\left[-\frac{E}{kT(t)}\right] \quad (2-15)$$

Equation (2-9) can be solved formally, giving

$$n_c(t) = m(t) - n_t(t) + m(0)(\rho - 1) \quad (2-16)$$

where

$$\rho = \frac{n_t(0) + n_c(0)}{m(0)} \quad (2-17)$$

and $n_t(0)$, $n_c(0)$, $m(0)$ are the initial electron and hole concentrations.

Substituting (2-16) into (2-10) we have

$$\frac{dm}{dt} = m(t) A [n_t(t) - (\rho - 1)m(0)] - Am^2(t) \quad (2-18)$$

Equation (2-18) is also a Bernoulli equation. Its solution is

$$m(t) = \frac{m(0) e^{u(t)}}{1 + Am(0) \int_0^t e^{u(t')} dt'} \quad (2-19)$$

where

$$u(t) = A \int_0^t [n_t(t') - m(0)(\rho - 1)] dt' \quad (2-20)$$

and $n_t(t)$ is given by (2-13).

The intensity of the thermoluminescence will be proportional to the rate of recombination, i.e., to dm/dt . Letting g be the proportionality constant which depends upon the geometry of the experiment, the

detection efficiency of the photomultiplier tube, etc., we have

$$I(t) = \frac{gAm(0) e^{u(t)}}{1 + Am(0) \int_0^t e^{u(t')} dt'} \times \left[n_t(t) + (1 - \rho)m(0) - \frac{m(0) e^{u(t)}}{1 + Am(0) \int_0^t e^{u(t')} dt'} \right] \quad (2-21)$$

Expression (2-21) gives the luminescence from a crystalline sample which has at time zero $n_t(0)$ trapped electrons and $m(0)$ recombination centers per unit volume as a result of some previous irradiation.

We turn now to a model for thermoluminescence based on a homogeneous sample of weakly interacting molecules. In this model, each molecule is presumed to act independently in the processes of absorbing, storing and re-emitting energy in the form of a photon.

There are several ways in which a molecule could trap and store energy. Perhaps the most familiar is the radiationless conversion from an excited singlet to excited triplet state which occurs in many aromatic molecules. The triplet state is metastable since the spin of the excited electron must be flipped during the triplet-singlet transition and the spin-orbit interaction which promotes this flipping is weak in these molecules. There are two difficulties with the hypothesis that a molecular triplet state is the metastable or trapping state required for thermoluminescence. One is the shortness of lifetime. Calculations of the lifetime of the triplet state in aromatic molecules have been made by McClure.⁸ Basing the calculation on the estimated spin-orbit coupling provided by the atom nearest the orbitals involved in the transition he

⁸D. S. McClure, J. Chem. Phys. 17, 905 (1949); 20, 682 (1952).

obtains lifetimes of 0.003, 0.0004, 0.0001 seconds when the coupling is due to a carbon, nitrogen or oxygen atom respectively. When molecular symmetry is taken in account there is some cancellation of this coupling and an increase in lifetime to as much as several seconds. The phenomenon of thermoluminescence, however, requires a metastable state with a lifetime several orders of magnitude longer, particularly at low temperature. This is the second difficulty. There is no theoretical justification for an assumption that the lifetime of the triplet state is strongly temperature dependent. Thus the triplet state does not have the necessary properties with regard to lifetime to be considered the metastable excited state involved in thermoluminescence.

One possibility for a molecular excited state with the required properties is the trapping of an excited electron by an ionic region of the molecule. For example, amino acids in water solution at physiological pH have both the amino and carboxyl groups ionized. Some small percentage of the molecules may also have this configuration in the dry state and thus have the ability to form the necessary metastable excited state. Let us call this conjecture the ionic trapping hypothesis.

Another possibility is suggested by the properties of certain ethylenic compounds.⁹ These molecules can form cis-trans isomeric states as the result of rotation about a carbon-carbon double bond. The potential energy of the two electrons involved in the π orbital of this double bond is a function of the angle of bond rotation as shown in Fig. 6. The curve labeled S gives the energy of the singlet state; the curve labeled T gives the energy of the triplet state as a function of bond rotation angle.

⁹C. Reid, Excited States in Chemistry and Biology (Butterworth, London, 1957).

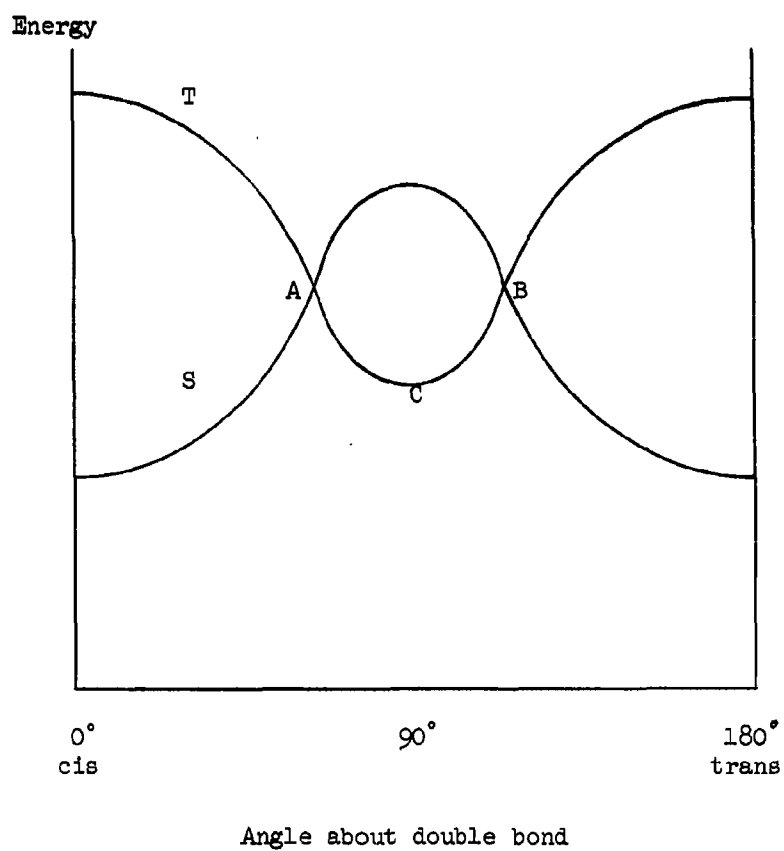


FIG. 6--Energy of singlet (S) and triplet (T) state orbitals as a function of the angle of twist about the axis of the ethylenic double bond (after Reid⁹).

The molecules investigated are in the singlet state before and after isomerization. Some but not all of them appear to undergo a singlet-triplet-singlet transition during the isomerization.

The reaction rate for the isomerization has the form

$$K = A \exp\left(-\frac{E}{kT}\right). \quad (2-22)$$

On the basis of experiments which determine A and E , the molecules investigated may be divided into two groups. (1) A group for which the activation energy is low and the frequency factor A is abnormally low, being about 10^4 sec^{-1} . (2) A group for which the activation energy is about twice as large as in the first group and the frequency factor is much closer to values found in most reactions, i.e., about 10^{11} . The interpretation is that the first group of molecules undergoes the isomerization via the singlet-triplet-singlet pathway. The required activation energy for this pathway is relatively low, and the forbiddenness of the singlet-triplet transition accounts for the low frequency factor. The second group isomerizes by going over the singlet state energy barrier.

An interesting feature of the first group is that at sufficiently low temperatures, molecules may become trapped in the intermediate 90° state at position C . The probability for such molecules to become untrapped is proportional to

$$\exp\left(-\frac{E_A - E_C}{kT}\right)$$

and thus has the temperature dependence needed for thermoluminescence. If such an isomerization effect is to explain thermoluminescence from amino acids, two additional assumptions must be made. One is that an

analogous isomerization effect may occur in some amino acids, say at the carbon-carbon bond linking the side group to the α -carbon. The second is that a photon will be given off at some point as the molecule goes from the metastable state (at position C) to the ground state at 0° to 180° . There is no evidence at present to substantiate either assumption. We call this possible explanation for amino acid thermoluminescence the frozen isomerization hypothesis.

Thirdly, it is possible that the necessary molecular trapping state is provided by a positive metal ion which is complexed with the molecule. A number of metal ions, e.g., iron, copper, have a strong tendency to complex with amino acids. Irradiation of such a complex at liquid nitrogen temperature may cause the formation of a stable charge-transfer complex. When the temperature is raised the transferred electron reverts back to an excited state of the molecule. From this state it undergoes a transition to the ground state with the emission of a photon. Let us call this the charge-transfer-complex hypothesis.

To derive an expression for the thermoluminescence intensity on the basis of a molecular model such as discussed above we begin by postulating that the transition rate for a molecule going from a metastable excited state to a short-lived (singlet or triplet) excited state and then to the ground state with the emission of a photon is

$$\omega = \gamma \exp\left(-\frac{E}{kT}\right) \quad (2-23)$$

where E is an activation energy and where γ contains the matrix element for the electronic transition. If there are n molecules per unit volume in the excited state, the number of radiative transitions expected during time dt is

$$-dn = n\gamma \exp\left[-\frac{E}{kT}\right] dt \quad (2-24)$$

The solution to this differential equation is

$$n(t) = n(0) \exp \left\{ - \gamma \int_0^t \exp \left[- \frac{E}{kT(t')} \right] dt' \right\}. \quad (2-25)$$

The intensity of the luminescence will be proportional to dn/dt . Thus

$$I(t) = gn(0)\gamma \exp \left(- \frac{E}{kT} \right) \exp \left\{ - \gamma \int_0^t \exp \left[- \frac{E}{kT(t')} \right] dt' \right\}. \quad (2-26)$$

The parameters E , γ which appear in this expression can be determined from the experimental curves in the following way. Let time $t = 0$ correspond to the beginning of the thermoluminescence. Then for times corresponding to the initial rise of the glow curve, the integral in (2-26) will be small and the luminescence will be given approximately by

$$I(t) = gn(0)\gamma \exp \left(- \frac{E}{kT} \right). \quad (2-27)$$

Using this region of the glow curve for a plot of $\ln I(t)$ vs $[1/T(t)]$ one obtains a straight line with slope $= -E/k$. At the peak of the glow curve,

$$T = T_p, \quad \frac{dT}{dt} = \left(\frac{dT}{dt} \right)_p \quad \text{and} \quad \frac{dI}{dt} = 0.$$

Differentiating (2-26) and introducing these peak conditions, one finds

$$\gamma = \frac{E}{kT_p^2} \left(\frac{dT}{dt} \right)_p \exp \left(\frac{E}{kT} \right) \quad (2-28)$$

These results will be used in the analysis of the experiments discussed in the next chapter. Equation (2-28) reveals another feature of the glow curves, namely, that the temperature at which the peak occurs depends on the heating rate. This is clearly seen in Fig. 7. A number of workers¹

¹D. Curie, op. cit.

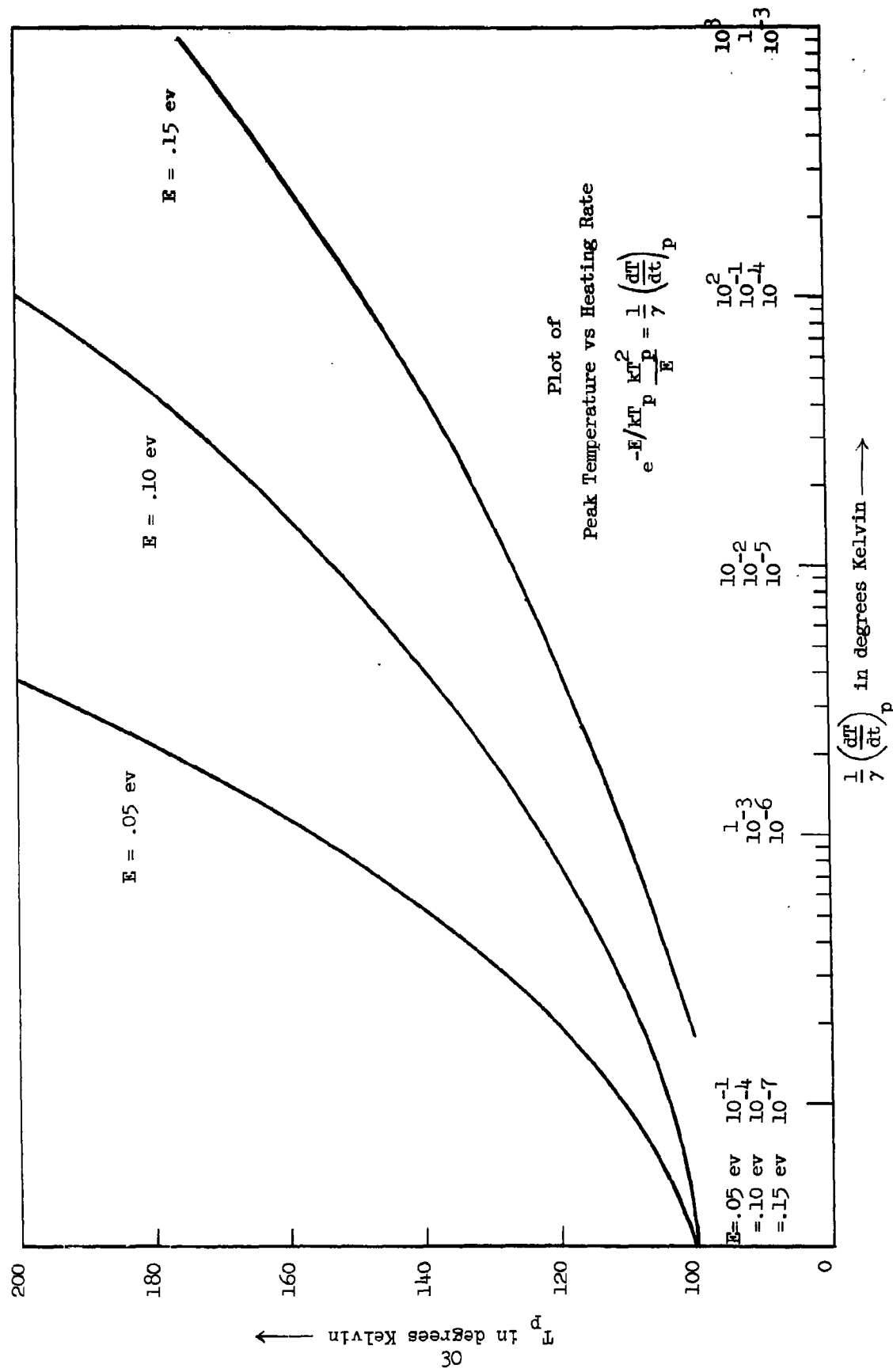


FIG. 7--The relationship between heating rate and peak temperature.

have attempted to use this fact to determine the constants E , γ .

Unfortunately this method lacks accuracy because T_p changes only slightly with dT/dt ; it is difficult to reduce the error below 20-30%.

Now we come to the mechanism proposed to account for thermoluminescence from polymers, more specifically from polypeptides. In this case, one imagines that irradiation of the molecules produces holes and trapped charges within the molecules. Irradiation causes a charge, say an electron, to be ejected from some site on the peptide; it is trapped at some other site. If the vacancy is represented by an open circle and the trapped electron by a closed circle, the polypeptide can now be represented as in Fig. 8.

These traps may be considered as regions of local polarization within the polypeptide. The site of the α -carbon of the amino acid, is likely to be such a region. To support this contention, there is the fact that amino acids, in water solution at physiological pH prefer the ionized structure about the α -carbon as discussed previously. Also, there is work of Box, Freund and Lilga¹⁰ showing that x-ray irradiation of some simple peptides produces dissociation of hydrogen from the α -carbon atom of the amino acid, and the work of Katayama and Gordy¹¹ showing that the α -carbon site is a trap for radiation damage. Let us assume that the polar environment of the α -carbons in the polypeptide serves to trap migrating electrons or holes.

The transition of a charge from one trap to the next is conceived of as a barrier penetration requiring a certain thermal activation energy.

¹⁰H. C. Box, H. G. Freund and K. Lilga, Symposium on Free Radicals in Biological Systems (ed. M. S. Blois, Academic Press, New York, 1961).

¹¹M. Katayama and W. Gordy, J. Chem. Phys. 35, 117 (1961).



FIG. 8--Block representation of a polypeptide. Each square represents a possible trapping site - one per amino acid. The black dot represents a trapped electron, the open circle is the corresponding hole.

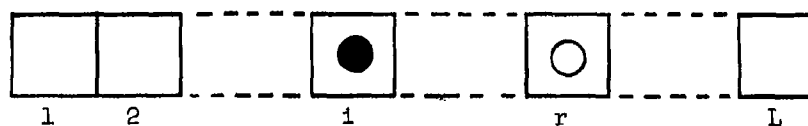


FIG. 9--Block representation of polypeptide showing the ordering of trapping sites used in the Markov analysis of charge migration.

It is expected that barriers within a polypeptide are more easily penetrated than barriers between two different polypeptides. For this reason, it is assumed that a charge will stay on one molecule, migrating along the molecule until it finds a hole with which it may recombine to produce a photon. It is further assumed, in the interest of simplification, that there is only one charge per molecule which, in fact, has been released from a trap site. Our model, then, consists of a single electron and a single hole constrained to a linear array of traps (finite in number). The electron hops from one trap to another but the hole remains fixed. The process continues until the electron and hole recombine. This migration process has the Markov property:¹² given the state of the molecule at any time, future changes are independent of the past. Let $P_{in}(\tau, t)$ be the conditional probability of finding the charge at the n th trapping site at time t given that at previous time the charge was at the i th trap. Then

$$P_{in}(\tau, t) = \sum_m P_{im}(\tau, s) P_{mn}(s, t) \quad \tau < s < t. \quad (2-29)$$

Next we postulate that for each trap in the molecule there exists a continuous function $C_m(t)$ which is the probability that an electron could escape from the m th trap during the time interval $t, t + \delta t$.

Thus

$$\lim_{\delta t \rightarrow 0} \frac{1 - P_{mm}(t, t + \delta t)}{\delta t} = C_m(t). \quad (2-30)$$

Furthermore, for any two traps m and n there exists a function $P_{mn}(t)$

¹²W. G. Feller, Introduction to Probability Theory and its Applications (Vol. 1, 2nd ed., Wiley, New York, 1957).

which is the conditional probability that if an electron escapes from trap m during $t, t + \delta t$ it is captured by trap n . Thus

$$\lim_{\delta t \rightarrow 0} \frac{P_{mn}(t, t + \delta t)}{\delta t} = C_m(t) p_{mn}(t) \quad m \neq n \quad (2-31)$$

with

$$\sum_n p_{mn} = 1, \quad p_{mm} = 0,$$

m, n finite. A stochastic process which conforms to these postulates can be described by the Kolomogorov equations

$$\frac{\partial}{\partial t} P_{in}(\tau, t) = -C_n(t) P_{in}(\tau, t) + \sum_{m \neq n} P_{im}(\tau, t) C_m(t) p_{mn}(t). \quad (2-32)$$

In this system of equations, i and t are fixed and the equations are actually ordinary differential equations.

A simple example will indicate how the glow curve may be obtained from the above. Assume the molecule has one trap and one recombination site, labelled 1 and 2 respectively. After the material has been irradiated, some molecules will have their traps occupied by electrons (and recombination sites occupied by holes). The probability per unit time that an electron will escape from the trap (when the material is warmed) is $c_1(t)$ while the probability per unit time that an electron will escape from a recombination site is zero, or $c_2(t) = 0$. Further, $p_{12}(t) = 1$, that is the electron, if it escapes from the trap, is certain to end up at the recombination site. $p_{21}(t)$ need not be specified.

Under these circumstances, the Kolomogorov equations take the simple form

$$\frac{\partial}{\partial t} P_{12}(\tau, t) = C_1(t) P_{11}(\tau, t) \quad (2-33)$$

$$\frac{\partial}{\partial t} P_{11}(\tau, t) = -C_1(t) P_{11}(\tau, t).$$

We note that for the simple case under consideration $P_{11}(\tau, t)$ represents the probability that a trapped electron has not recombined. Hence the number of molecules per unit volume having traps occupied by electrons at time t is

$$n(t) = n(\tau)P_{11}(\tau, t) \quad (2-35)$$

where $n(\tau)$ is the initial concentration of molecules with trapped charges. Hence Eq. (2-34) may be written

$$\frac{d}{dt} n(t) = -C_1(t)n(t) \quad (2-36)$$

If $C_1(t)$ is known, Eq. (2-36) gives the glow curve since the intensity of the emitted light is proportional to dn/dt . Suppose that the removal of an electron from a trap involves a thermal activation energy E . Then

$$C_1(t) = \gamma \exp\left[-\frac{E}{kT(t)}\right], \quad (2-37)$$

which depends on time only to the extent that the temperature T may depend on time. We have then, for the glow curve,

$$I(t) = gn(\tau)\gamma \exp\left(-\frac{E}{kT}\right) \exp\left[-\gamma \int_{\tau}^t \exp\left(-\frac{E}{kT} dt'\right)\right] \quad (2-38)$$

which is the same as (2-26). This is to be expected since the same physical picture is used in the derivation of both equations. For the general case we consider a linear polymer, l units long, containing one trapped electron and one recombination site. The electron may be trapped in any one of $l-1$ sites, from which it can escape, or in the one recombination site from which it cannot escape. Thus, as shown in Fig. 9, the electron is in trap i and the recombination site is at r . As the material is warmed, it is assumed that the electron may hop from

i to either $i + 1$ or $i - 1$. The process continues, by a succession of hops to neighboring sites, until the electron finds the site r , recombination takes place and a photon is emitted.

In order to obtain the glow curve we need to know $dn(t)/dt$ where $n(t)$ is the total number of molecules per unit volume containing a trapped electron at time t . We proceed as follows: Let $n_{ir}(\tau)$ be the concentration of molecules at initial time with electron at i , recombination site at r . The number of these molecules which at time t still have a trapped electron but not necessarily at i , is

$$n_{ir}(t) = n_{ir}(\tau) \sum_{m < r} P_{im}(\tau, t). \quad (2-39)$$

The number of molecules per unit volume, $n(t)$ having an electron in some trap and a recombination site at any of the i possible sites is obtained by summing $n_{ir}(t)$ over i and r . That is

$$n(t) = \sum_{r=2}^L \sum_{i < r} n_{ir}(t). \quad (2-40)$$

The counting scheme used is responsible for the summation over recombination sites beginning at 2. We assume that all initial arrangements of trapped electron and recombination sites are equally probable, i.e.,

$$n_{ir}(\tau) = n_0 \quad (2-41)$$

where n_0 is a constant, the same for all r and all $i < r$.

Recall that the equations for the conditional probability $P_{im}(\tau, t)$ are

$$\frac{\partial}{\partial t} P_{im}(\tau, t) = -C_m(t)P_{im}(\tau, t) + \sum_{k \neq m} P_{ik}(\tau, t)C_k(t)P_{km} \quad (2-42)$$

with $m = 1, 2, \dots, r-1$. The assumption that when a trapped electron

escapes it will be retrapped by one of its two nearest neighbors gives

$$P_{km} = \frac{1}{2} \text{ when } |k - m| = 1 \quad (2-43)$$

except

$$P_{12} = 1 \quad (2-44)$$

with

$$P_{km} = 0 \quad (2-45)$$

otherwise.

Next we assume that the escape probability $C_m(t)$ is the same for all traps, while for the recombination site r , $C_r(t) = 0$. Let

$$C_m(t) = C(t), \quad m = 1, 2, \dots, r-1. \quad (2-46)$$

Now using (2-43), (2-44), (2-45), (2-46), we can write the set of equations (2-42) in vector form

$$\frac{\partial}{\partial t} \begin{vmatrix} P_{i1}(\tau, t) \\ P_{i2}(\tau, t) \\ . \\ . \\ . \\ . \\ P_{ir-1}(\tau, t) \end{vmatrix} = C(t) \begin{vmatrix} -1 & \frac{1}{2} & & & & \\ 1 & -1 & \frac{1}{2} & & & \\ & \frac{1}{2} & -1 & . & & \\ & & . & . & . & \\ & & & . & . & . \\ & & & & . & . & . \\ & & & & & . & -1 & \frac{1}{2} \\ & & & & & & \frac{1}{2} & -1 \end{vmatrix} \begin{vmatrix} P_{i1}(\tau, t) \\ P_{i2}(\tau, t) \\ . \\ . \\ . \\ . \\ P_{ir-1}(\tau, t) \end{vmatrix} \quad (2-47)$$

The substitution

$$P_{im}(\tau, t) = U_{im}(t) \exp \left[- \int_{\tau}^t C(t') dt' \right] \quad (2-48)$$

simplifies the matrix involved in this equation and gives the following

vector equation for the $U_{im}(t)$.

$$\frac{\partial}{\partial t} \begin{pmatrix} U_{11}(t) \\ U_{12}(t) \\ . \\ . \\ . \\ . \\ U_{1r-1}(t) \end{pmatrix} = C(t) \begin{pmatrix} 0 & \frac{1}{2} & & & & \\ 1 & 0 & \frac{1}{2} & & & \\ & \frac{1}{2} & 0 & . & & \\ & & . & . & . & \\ & & & . & . & . \\ & & & & . & . \\ & & & & & \frac{1}{2} \\ & & & & & 0 \end{pmatrix} \begin{pmatrix} U_{11}(t) \\ U_{12}(t) \\ . \\ . \\ . \\ . \\ U_{1r-1}(t) \end{pmatrix} \quad (2-49)$$

If we denote the matrix in (2-49) by B_r , this equation can be written more compactly as

$$\frac{\partial}{\partial t} \overrightarrow{U_i(t)} = C(t) B_r \overrightarrow{U_i(t)} . \quad (2-50)$$

The initial conditions for the $U_{im}(t)$ are

$$U_{im}(\tau) = \delta_{im} \quad (2-51)$$

To solve (2-50) we find the matrices A_r , A_r^{-1} such that

$$A_r^{-1} B_r A_r = D_r \quad (2-52)$$

where D_r is the $(r-1) \times (r-1)$ diagonal matrix whose diagonal elements $\lambda_1, \lambda_2, \dots, \lambda_{r-1}$ are the eigenvalues of B_r . We assume that B_r can always be diagonalized. This has been verified for $r \leq 7$ by noting that q_r , the characteristic polynomial of B_r , satisfies the recursion relation $q_r = -\lambda q_{r-1} - \frac{1}{4} q_{r-2}$ with $q_0 = 2$, $q_1 = -\lambda$, and using this relation to find q_r and its roots. We now write (2-50) as

$$\frac{\partial}{\partial t} A_r^{-1} \overrightarrow{U_i(t)} = C(t) A_r^{-1} B_r A_r A_r^{-1} \overrightarrow{U_i(t)}$$

or

$$\frac{\partial}{\partial t} \overrightarrow{V_1(t)} = C(t) D_r \overrightarrow{V_1(t)} \quad (2-53)$$

where

$$\overrightarrow{V_1(t)} = A_r^{-1} \overrightarrow{U_1(t)} . \quad (2-54)$$

Equation (2-53) can be solved immediately. We have

$$\overrightarrow{V_1(t)} = E_r(t) \overrightarrow{V_1(\tau)} \quad (2-55)$$

where $E_r(t)$ is the diagonal matrix

$$E_r(t) = \begin{vmatrix} e^{\lambda_1 J} & & & \\ & e^{\lambda_2 J} & & \\ & & \ddots & \\ & & & e^{\lambda_{r-1} J} \end{vmatrix}$$

with

$$J = \int_{\tau}^t C(t') dt' . \quad (2-56)$$

The initial values of the $\overrightarrow{V_{im}(t)}$ are given by

$$\overrightarrow{V_{im}(\tau)} = A_r^{-1} \overrightarrow{U_1(\tau)} . \quad (2-57)$$

The solution to Eq. (2-50) may now be written

$$\overrightarrow{U_1(t)} = A_r E_r(t) A_r^{-1} \overrightarrow{U_1(\tau)} \quad (2-58)$$

and

$$\overrightarrow{P_1(\tau, t)} = e^{-J} \overrightarrow{U_1(t)} . \quad (2-59)$$

$n(t)$ may now be computed from Eqs. (2-39), (2-40) and (2-59). Specifically,

we have

$$n(t) = n(\tau) \sum_{r=2}^L \left[\sum_{1 \leq m} \sum_{m \leq r} P_{1m}(\tau, t) \right] \quad (2-60)$$

where the double sum inside the parenthesis is equal to the sum of all the elements in $A_r E_r(t) A_r^{-1}$.

The special case $L = 4$ provides an example of this technique.

Consider first the subcase $r = 4$. The matrix B_4 is

$$B_4 = \begin{vmatrix} 0 & \frac{1}{2} & 0 \\ 1 & 0 & \frac{1}{2} \\ 0 & \frac{1}{2} & 0 \end{vmatrix}.$$

The eigenvalues of this matrix are

$$\lambda_1 = 0, \quad \lambda_2 = \frac{\sqrt{3}}{2}, \quad \lambda_3 = -\frac{\sqrt{3}}{2}.$$

The matrices A_4 , A_4^{-1} are found, using standard techniques, to be

$$A_4 = \begin{vmatrix} -1 & 1 & 1 \\ 0 & \sqrt{3} & -\sqrt{3} \\ 2 & 1 & 1 \end{vmatrix}$$

$$A_4^{-1} = \frac{1}{6} \begin{vmatrix} -2 & 0 & 2 \\ 2 & \sqrt{3} & 1 \\ 2 & -\sqrt{3} & 1 \end{vmatrix}.$$

The matrix $E_4(t)$ is

$$E_4(t) = \begin{vmatrix} 1 & 0 & 0 \\ 0 & e^{\frac{\sqrt{3}}{2} J} & 0 \\ 0 & 0 & e^{-\frac{\sqrt{3}}{2} J} \end{vmatrix}.$$

The sum of all elements in $A_4 E_4(t) A_4^{-1}$ is

$$\frac{9 + 5\sqrt{3}}{6} \exp\left(\frac{\sqrt{3}}{2} J\right) + \frac{9 - 5\sqrt{3}}{6} \exp\left(-\frac{\sqrt{3}}{2} J\right).$$

The contribution to $n(t)$ from subcase $r = 4$ is

$$n_0 e^{-J} \left[\frac{9 + 5\sqrt{3}}{6} \exp\left(\frac{\sqrt{3}}{2} J\right) + \frac{9 - 5\sqrt{3}}{6} \exp\left(-\frac{\sqrt{3}}{2} J\right) \right]. \quad (2-61)$$

Next consider subcase $r = 3$. The matrix B_3 is

$$B_3 = \begin{vmatrix} 0 & \frac{1}{2} \\ 1 & 0 \end{vmatrix}.$$

The eigenvalues of B_3 are

$$\lambda_1 = \frac{1}{\sqrt{2}}, \quad \lambda_2 = -\frac{1}{\sqrt{2}}.$$

The matrices A_3 , A_3^{-1} , $E_3(t)$ are

$$A_3 = \begin{vmatrix} 1 & 1 \\ \sqrt{2} & -\sqrt{2} \end{vmatrix} \quad A_3^{-1} = \frac{1}{2} \begin{vmatrix} 1 & \frac{1}{\sqrt{2}} \\ 1 & -\frac{1}{\sqrt{2}} \end{vmatrix}$$

$$E_3(t) = \begin{vmatrix} e^{\frac{1}{\sqrt{2}} J} & 0 \\ 0 & e^{-\frac{1}{\sqrt{2}} J} \end{vmatrix}.$$

The sum of all elements in $A_3 E_3(t) A_3^{-1}$ is

$$\left(1 + \frac{3}{2\sqrt{2}}\right) \exp\left(\frac{1}{\sqrt{2}} J\right) + \left(1 - \frac{3}{2\sqrt{2}}\right) \exp\left(-\frac{1}{\sqrt{2}} J\right).$$

The contribution to $n(t)$ from subcase $r = 3$ is therefore

$$n_0 e^{-J} \left[\left(1 + \frac{3}{2\sqrt{2}}\right) \exp\left(\frac{1}{\sqrt{2}} J\right) + \left(1 - \frac{3}{2\sqrt{2}}\right) \exp\left(-\frac{1}{\sqrt{2}} J\right) \right]. \quad (2-62)$$

The last subcase is $r = 2$. This case is simply the solution to (2-36) with

$$C_1(t) = C(t) .$$

The contribution is

$$n_0 e^{-J} . \quad (2-63)$$

Putting together the contributions [(2-61), (2-62) and (2-63)] of the subcases we get the number of molecules per unit volume with trapped electrons at time t .

$$n(t) = n_0 e^{-J} \left[\left(1 + \frac{3}{2\sqrt{2}} \right) \exp\left(\frac{1}{\sqrt{2}} J\right) + \left(1 - \frac{3}{2\sqrt{2}} \right) \exp\left(-\frac{1}{\sqrt{2}} J\right) + \frac{9 + 5\sqrt{3}}{6} \exp\left(\frac{\sqrt{3}}{2} J\right) + \frac{9 - 5\sqrt{3}}{6} \exp\left(-\frac{\sqrt{3}}{2} J\right) \right] , \quad (2-64)$$

with

$$J = \int_{\tau}^t C(t') dt' .$$

Recall that $C(t)$ is the transition frequency for an electron to escape from a trap. Two expressions for $C(t)$ derived by Kubo are presented as Eqs. (A-8) and (A-9) in Appendix I. To decide which is pertinent for trapping in polypeptides, we need to know the vibrational frequency of the skeletal atoms of the molecule. Infrared absorption data¹³ suggest that the frequency is roughly $2 \times 10^{13} \text{ sec}^{-1}$. This corresponds to vibrational quantum of $h\nu 9 \cdot 10^{-2} \text{ ev}$. Thus at liquid nitrogen temperature, $h\nu/kT \approx 10$ and the first expression (A-8) is correct. We have

$$C(t) = \gamma \exp\left(-\frac{E}{kT}\right).$$

¹³P. Doty and E. P. Geiduschek, "Optical Properties of the Proteins" in Proteins, edited by H. Neurath and K. Bailey, Vol. 1, part A (Academic Press, Inc., New York, 1953).

The thermoluminescence intensity is proportional to $-dn/dt$ so that

$$I(t) = gn(\tau)\gamma \exp\left[-\frac{E}{kT(t)}\right] \left\{ \exp[-J(t)] + \left(\frac{1}{4} + \frac{1}{2\sqrt{2}}\right) \exp\left[\left(\frac{1}{\sqrt{2}} - 1\right)J(t)\right] + \left(\frac{1}{4} - \frac{1}{2\sqrt{2}}\right) \exp\left[-\left(\frac{1}{\sqrt{2}} + 1\right)J(t)\right] + \left(\frac{1}{4} + \frac{\sqrt{3}}{6}\right) \exp\left[\left(\frac{\sqrt{3}}{2} - 1\right)J(t)\right] + \left(\frac{1}{4} - \frac{\sqrt{3}}{6}\right) \exp\left[-\left(\frac{\sqrt{3}}{2} + 1\right)J(t)\right] \right\} \quad (2-65)$$

with

$$J(t) = \gamma \int_{\tau}^t \exp\left(-\frac{E}{kT(t')}\right) dt' .$$

Equation (2-65) represents the glow curve from a polymer with one recombination site and three charge-trapping sites. It may be compared with (2-38) which represents the glow curve from a molecule having one recombination site and one electron-trapping site. Such a comparison is made graphically in Fig. 25.

To summarize, in order for a substance to exhibit thermoluminescence, it or its constituent molecules must possess metastable excited states which have two properties. (1) The transition rate from the metastable excited state to a short-lived excited state must increase markedly with temperature. (2) The transition from this excited state to the ground state must be accompanied by the creation of a photon. The glow curve is proportional to the time rate of change of the number of electrons or molecules in metastable excited states. The problem of deriving a formula for the glow curve is essentially one of finding this function.

Glow curve derivations have been made in terms of three different models. (1) The semiconductor model involving valence and conduction bands with traps for electrons and holes in the energy gap. (2) The

monomolecular model in which the molecules of the solid have a metastable excited state whose lifetime decreases strongly as the temperature of the sample is increased. (3) The intramolecular charge-migration model. In this model the mean time for steps in the migration process decreases strongly as the temperature increases. The first derivation uses some points of view and results of Halperin and Braner.⁴ The second derivation has been made by a number of workers. The third is believed to be a new result.

⁴A. Halperin and A. A. Braner, Phys. Rev. 117, 408 (1960).

CHAPTER III

RESULTS AND INTERPRETATION OF THERMOLUMINESCENCE EXPERIMENTS

Thermoluminescence measurements have been made in the following way. The sample - typically 100 mg of powder or 1 ml of liquid - is placed on a copper sample plate and covered with a quartz cover glass. A copper constantan thermocouple is attached to the sample plate and the plate is fastened to the heater. The heater is mounted inside a Dewar and is cooled to 77° K by pouring liquid nitrogen into the Dewar - see Figs. 10 and 11. Dry nitrogen gas is fed into the Dewar to flush out water vapor, thus preventing moisture condensation on the quartz cover glass. After the sample is cooled to 77° K it is irradiated with ultraviolet light from a Hanovia model 30600 lamp. There is a band pass filter, consisting of 2 Corning glass filters, CS numbers 9-54 and 7-54, between the ultraviolet lamp and the sample. The transmission range of this filter is 2500 Å to 3900 Å. After the sample has received 10^{10} ergs of radiant energy, the lamp and filter are removed and a photomultiplier tube is placed over the sample. The heater current is turned on and the photomultiplier current and sample temperature are measured as a function of time.

Figure 12 is a block diagram of the apparatus used for thermoluminescence experiments. Figure 13 is a photograph of the cryostat beneath the photomultiplier tube enclosure. Figure 14 is a photograph of the entire apparatus. The high voltage supply is a Baird Atomic power supply, model 312A. It supplies voltage to a DuMont No. 6292 photomultiplier tube. The light pipe is a 4" length of polished lucite rod, $1\frac{1}{2}$ " in diameter. The Keithley model 150 AR microvolt ammeter amplifies the current output

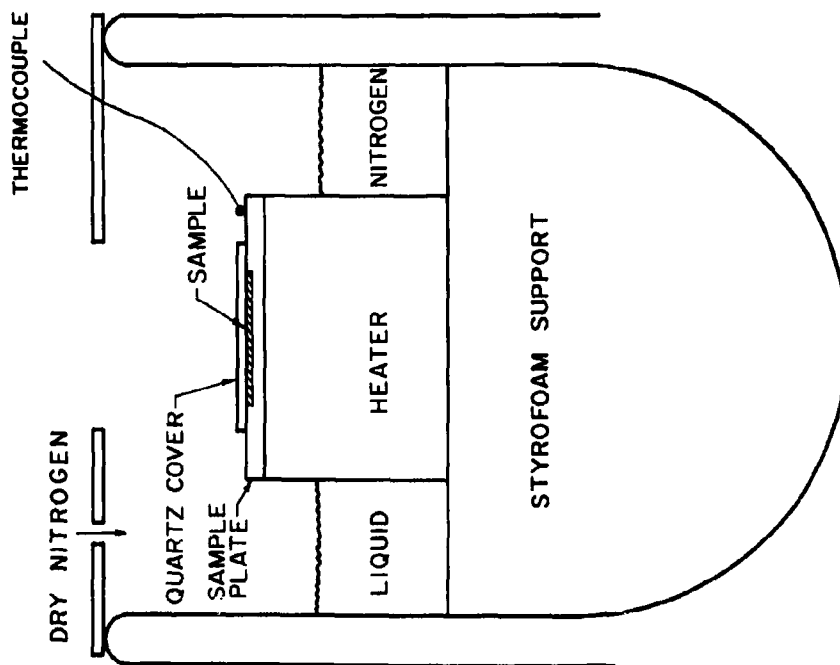


FIG. 10--Cross section of the thermoluminescence cryostat. The ultraviolet lamp and the photomultiplier tube are positioned consecutively over the opening above the sample.

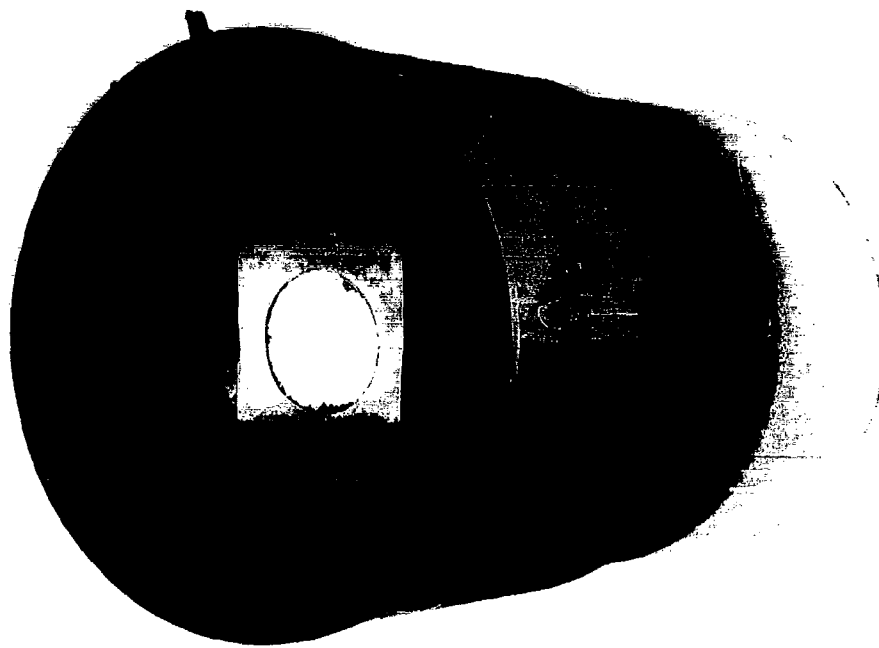


FIG. 11--Top view of the thermoluminescence cryostat showing the inlet for the dry nitrogen gas, the thermocouple lead and the ac cord to the heater. The white powder inside is a typical sample, held in place by a quartz cover glass. The quartz glass is in turn held in place by a thin aluminum plate which may be seen immediately around the sample material.

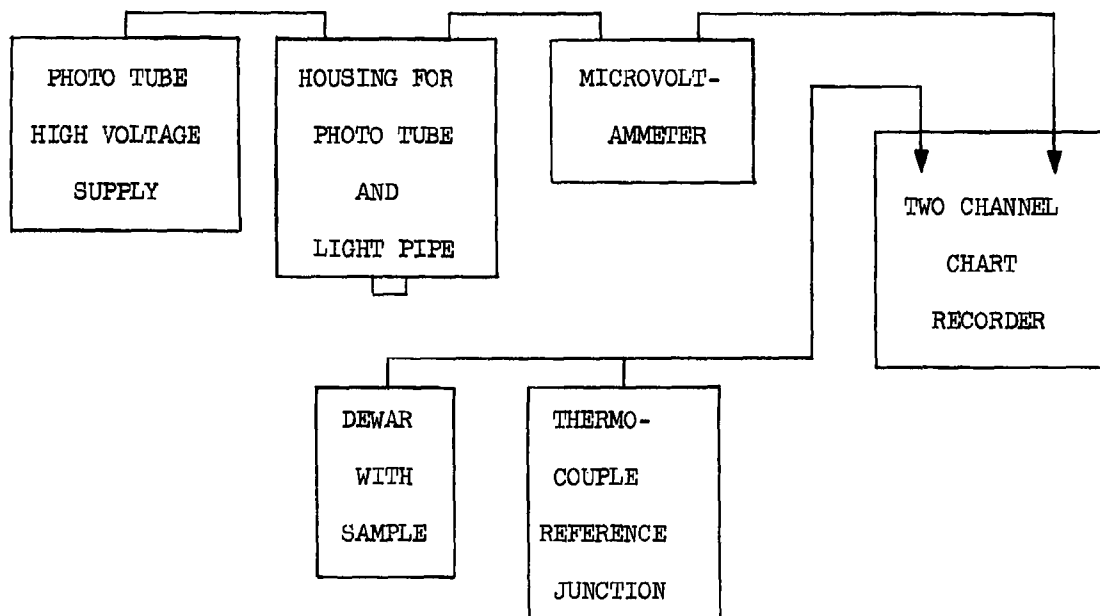


FIG. 12--A block diagram of the thermoluminescence apparatus.

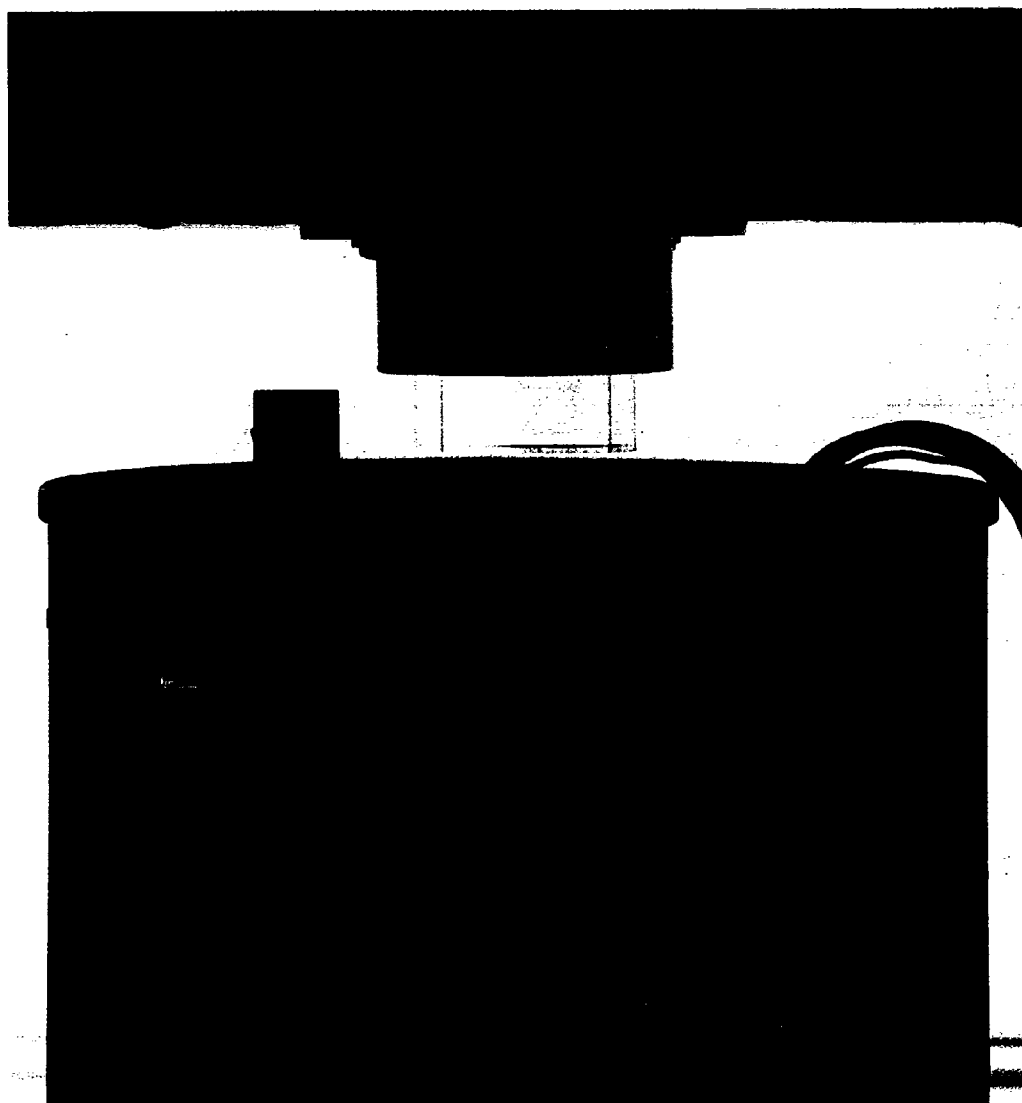


FIG. 13--Side view of the cryostat in position under the black box containing the photomultiplier tube. One end of the lucite light pipe leading to the photomultiplier tube may be seen over the cryostat opening.

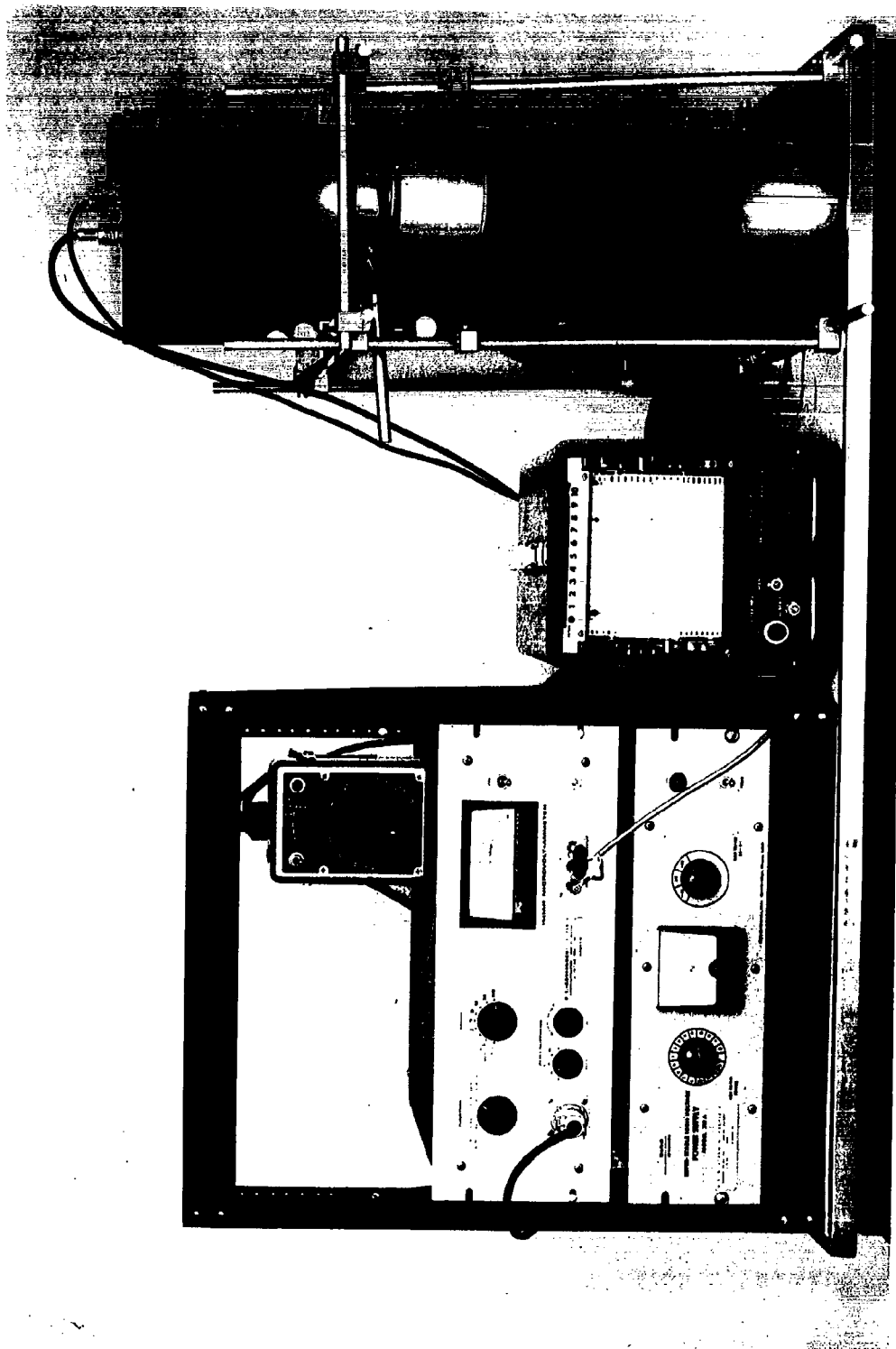


FIG. 14--The thermoluminescence apparatus as described in the text with the cryostat in position beneath the ultraviolet lamp. The small Dewar is the water and ice reference junction. The black felt skirt hanging down from the black box keeps extraneous light from reaching the photomultiplier tube during thermoluminescence measurements.

of the photomultiplier tube and drives the B22 input channel of the Varian Associates model G22 dual channel recorder. The emf of the sample thermocouple is balanced against the emf from the crushed ice and water reference junction and fed to the A-22-A input channel of the chart recorder. This input is adjusted so that the recorded thermocouple emf agrees with that measured with a Rubicon model 2732 Potentiometer. The thermocouple emf at liquid nitrogen temperature agrees with the published values¹ to within 0.5%.

Voltage across the sample heater is regulated by a Variac. The sample materials were obtained from the California Corporation for Biochemical Research (CCBR) or from Nutritional Biochemicals Corporation (NBCo) except where otherwise indicated.

Data as supplied by the chart recorder consist of the current output of the photomultiplier tube and the balanced thermocouple output plotted as a function of time. From these data a plot of the luminescence and the temperature as a function of time, can be obtained. Figure 15 shows such a plot made from the thermoluminescence data for L-tyrosine. This glow curve can be analyzed in terms of the simple monomolecular kinetics developed in the previous chapter. To review briefly, the basic assumption was that each molecule of the sample acted independently in storing and releasing energy. It followed that if the probability per unit time for emission of a photon were

$$\omega(t) = \gamma \exp\left[-\frac{E}{kT(t)}\right]$$

¹F. A. Mauer, "Low Temperature Equipment and Techniques" in Formation and Trapping of Free Radicals, edited by A. M. Bass and H. P. Broida, (Academic Press, New York, 1960).

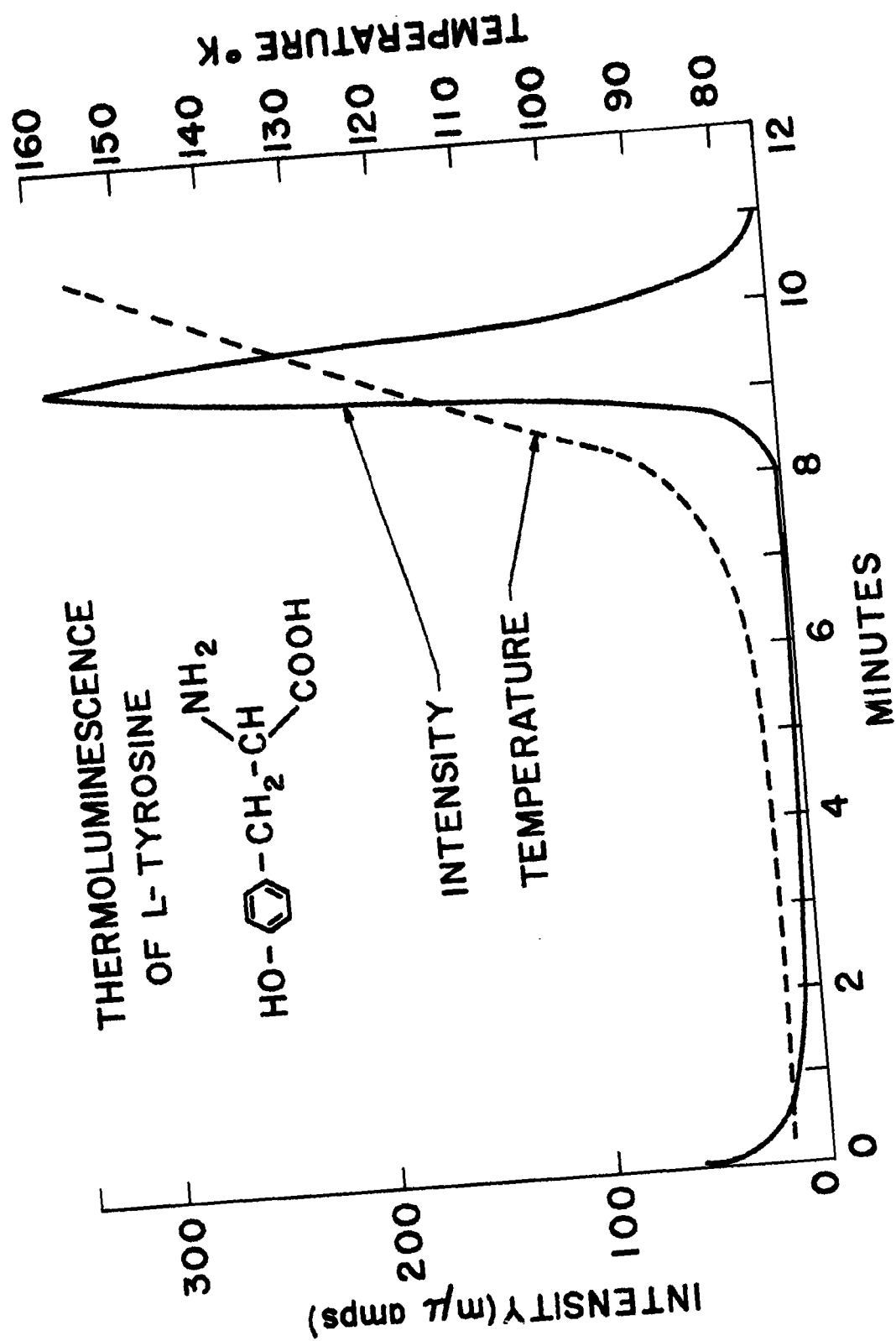


FIG. 15--Typical glow curve of uv irradiated L-tyrosine.
The temperature at the peak is 124° K.

then the thermoluminescence intensity as a function of time would be

$$I(t) = gn(0)\gamma \exp\left[-\frac{E}{kT(t)}\right] \exp\left\{-\gamma \int_0^t \exp\left[-\frac{E}{kT(t')}\right] dt'\right\}. \quad (2-26)$$

The time $t = 0$ may be chosen to correspond to the beginning of the glow curve. Then during the initial rise in thermoluminescence intensity, the integral in (2-26) will be small, the exponential containing it will be essentially unity, and (2-26) can be approximated, after taking logarithms as

$$\ln[I(t)] \approx \text{constant} - \frac{E}{kT(t)}.$$

Figure 16 shows a logarithmic plot of the intensity of the beginning of the tyrosine glow curve as a function of the reciprocal of the temperature in degrees Kelvin. The activation energy obtained from the slope of the line drawn through these points is 0.155 ± 0.015 ev. The peak temperature, T_p , is 124° K; the heating rate at the peak is 26° K min⁻¹. Putting these numbers into Eq. (2-28) we get the frequency factor $\gamma = 1.3 \cdot 10^5$ sec⁻¹.

A number of amino acids and other molecules closely related to them have been investigated and the thermoluminescence data, when obtained, analyzed as shown above. Table I contains the averaged results of these experiments. Tyrosine and phenylalanine which are discussed in detail in this chapter are included in the table for the sake of completeness. Samples of the same compound from different biochemical supply houses show in some cases different responses. The source of the sample has therefore been included in the table.

The glow curve of CCB L-phenylalanine (Fig. 17) has two peaks and a strong initial luminescence or phosphorescence subsequent to its

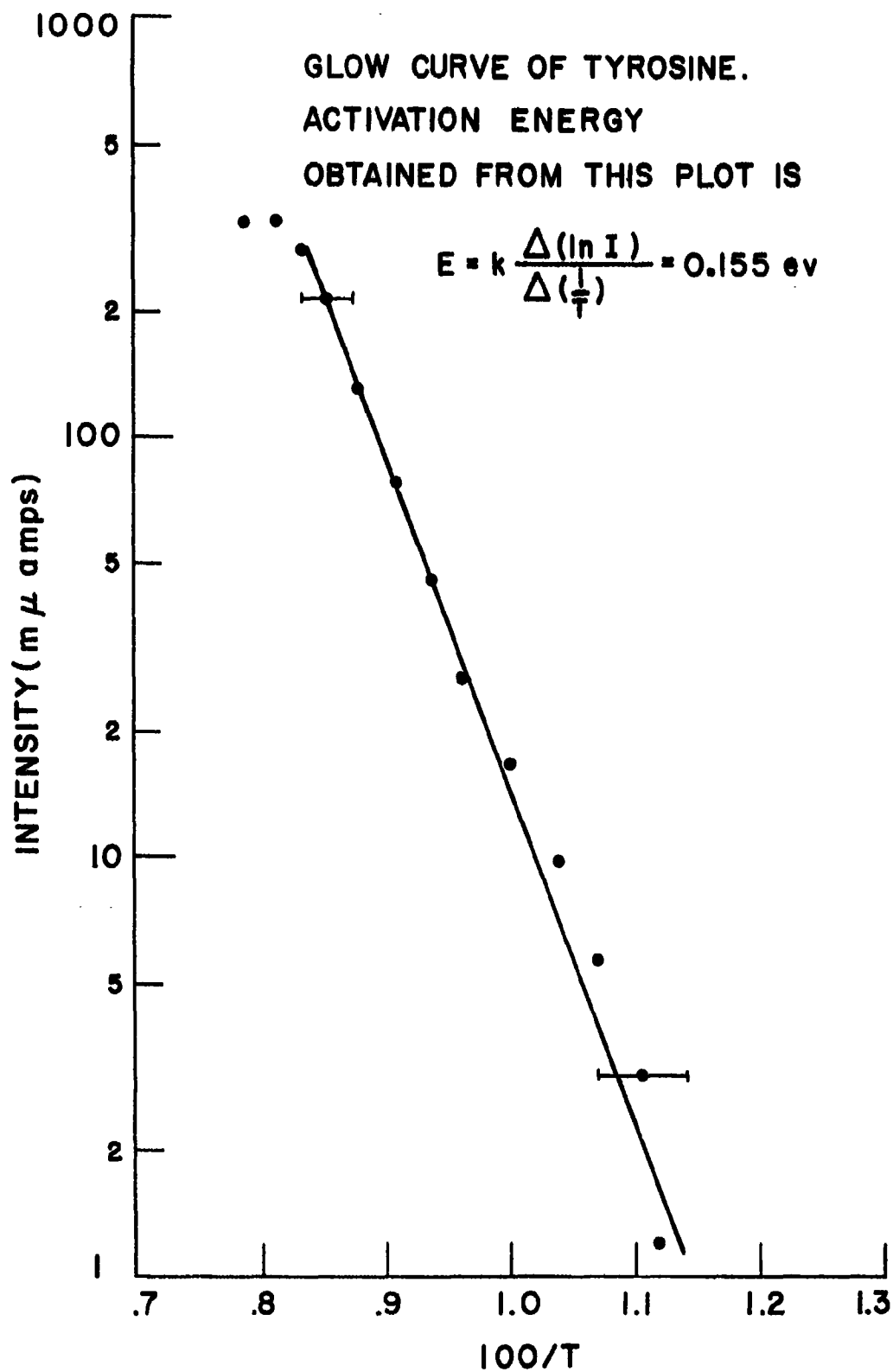


FIG. 16--Semilogarithmic plot of intensity versus 100/T for the initial part of the tyrosine glowcurve. Uncertainty in temperature measurement is indicated by the error bars.

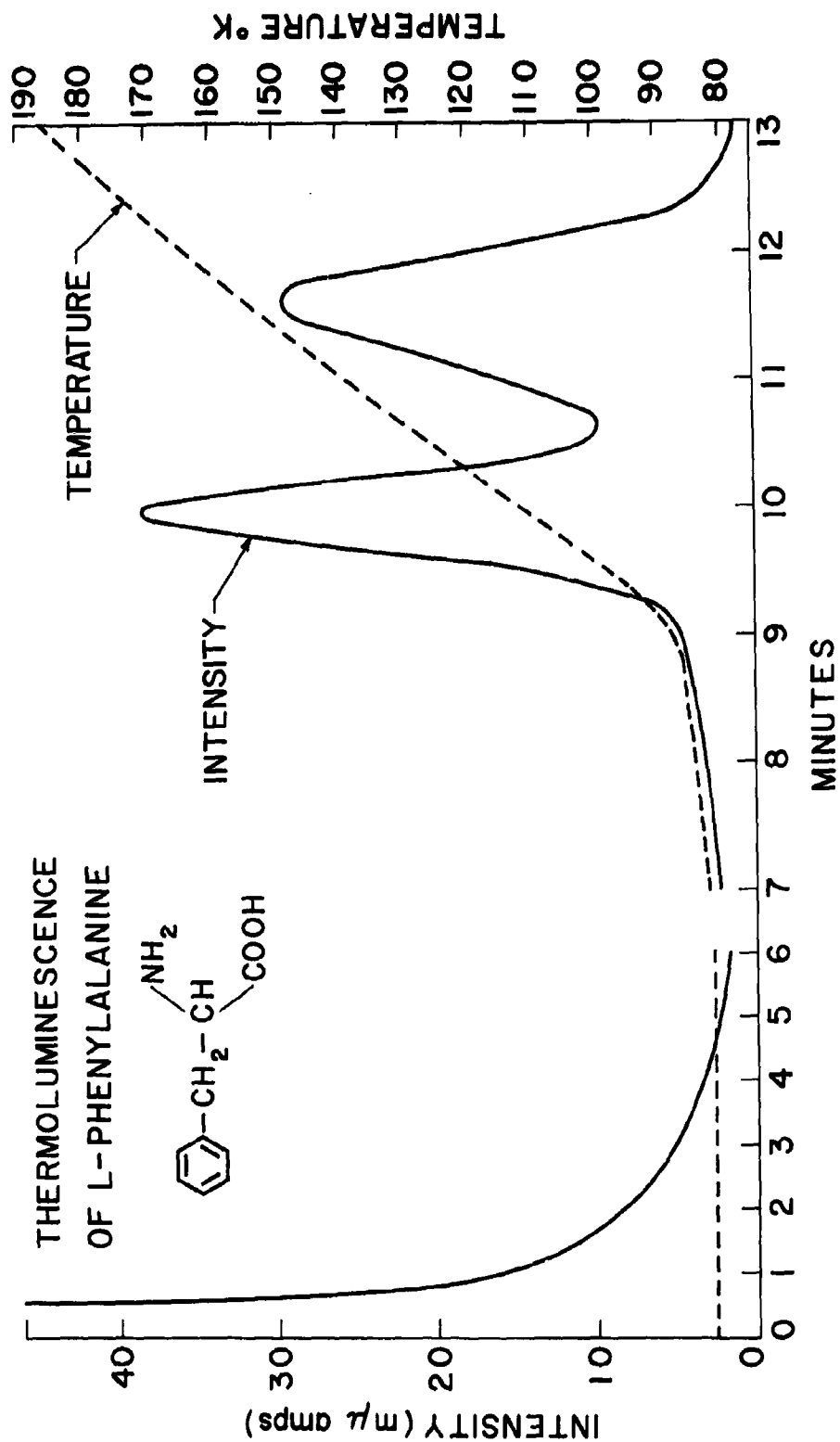


FIG. 17--Typical glow curve of uv irradiated L-phenylalanine.
 The peak temperatures are 113° K and 155° K.

TABLE 1

This table lists the amino acids and closely related molecules which have been investigated for thermoluminescence. All samples were in polycrystalline form. All were cooled to liquid nitrogen temperature, irradiated with uv and subsequently heated and looked at for evidence of thermoluminescence as described in the text. The first column of this table gives the name of the compound, the source, the side group or the structure if the compound is not an amino acid. The second column gives the maximum thermoluminescence intensity in units of millimicroamps, the observed photomultiplier current. Column 3 gives the temperature at the peak, or peaks if there is more than one and they are reasonably well resolved. Columns 4 and 5 give the activation energy and frequency factor, determined in the way described in the text whenever this has been possible.

COMPOUND, SOURCE AND STRUCTURE OR SIDE GROUP	TL INTENSITY IN mμ AMP	T _p °K	E ev	γ min ⁻¹
Glycine (CCBR) H-	< 1	-	-	-
L-Alanine (CCBR) CH ₃ -	3	112±5	TL too weak for analysis	
L-Serine (CCBR) CH ₂ OH-	< 1	-	-	-
L-Threonine (CCBR) CH ₃ CHOH-	< 1	-	-	-
L-Valine (CCBR) $\begin{array}{c} \text{CH}_3 \backslash \\ \text{CH} - \\ / \text{CH}_3 \end{array}$	~ 1	109±5	TL too weak for analysis	
	55			

TABLE 1 (Continued)

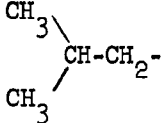
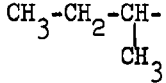
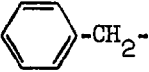
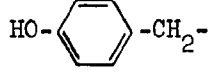
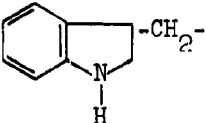
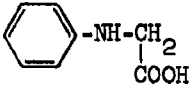
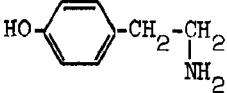
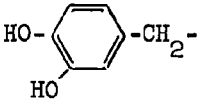
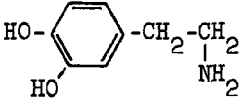
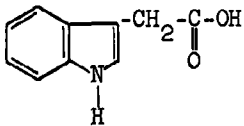
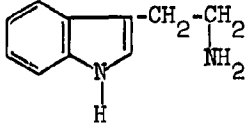
COMPOUND, SOURCE AND STRUCTURE OR SIDE GROUP	TL INTENSITY IN mμ AMP	T _p °K	E ev	γ min ⁻¹
L-Leucine (CCBR)	< 1	-	-	-
				
L-Isoleucine (CCBR)	< 1	-	-	-
				
L-Phenylalanine (CCBR)	38	113	.086±.015	4.10 ⁴
	29	155	.22±.06	~5.10 ⁷
L-Phenylalanine (NBCo)	60	123	.11±.015	8.10 ⁴
(Same side group)				
D-Phenylalanine (CCBR)	< 1	-	-	-
(Same side group)				
D-Phenylalanine (NBCo)	< 1	-	-	-
(Same side group)				
L-Tyrosine (CCBR)	340	124	.155±.015	8.10 ⁶
				
L-Cysteine.HCl (CCBR)	< 1	-	-	-
HS-CH ₂ -				
L-Methionine (CCBR)	< 1	-	-	-
CH ₃ -S-CH ₂ -CH ₂				
L-Tryptophan (CCBR)	9	115	TL too weak for analysis; peaks were not well separated.	
	10	152		

TABLE 1 (Continued)

COMPOUND, SOURCE AND STRUCTURE OR SIDE GROUP	TL INTENSITY IN mμ AMP	T _p °K	E _{ev}	γ min ⁻¹
L-Proline (CCBR) $ \begin{array}{c} \text{H}_2\text{C} - \text{CH}_2 \\ \quad \\ \text{H}_2\text{C} - \text{CH} - \text{COOH} \\ \\ \text{N} \\ \\ \text{H} \end{array} $	1	115±5	TL too weak for analysis	
L-Hydroxyproline (CCBR) $ \begin{array}{c} \text{H} \\ \\ \text{HO} - \text{C} - \text{CH}_2 \\ \quad \\ \text{H}_2\text{C} - \text{CH} - \text{COOH} \\ \\ \text{N} \\ \\ \text{H} \end{array} $	< 1	-	-	-
L-Histidine (CCBR) $ \begin{array}{c} \text{HC} = \text{C} - \text{CH}_2 - \\ \quad \\ \text{N} \quad \text{NH} \\ \backslash \quad / \\ \text{C} \\ \\ \text{H} \end{array} $	< 1	-	-	-
L-Aspartic Acid (CCBR) $ \begin{array}{c} \text{HO} - \text{C} - \text{CH}_2 - \\ \\ \text{O} \end{array} $	< 1	-	-	-
L-Glutamic Acid (CCBR) $ \begin{array}{c} \text{HO} - \text{C} - \text{CH}_2 - \text{CH}_2 - \\ \\ \text{O} \end{array} $	< 1	-	-	-
L-Arginine (CCBR) $ \begin{array}{c} \text{H}_2\text{N} - \text{C} - \text{NH} - (\text{CH}_2)_3 - \\ \\ \text{NH} \end{array} $	< 1	-	-	-
L-Lysine (CCBR) $ \text{H}_2\text{N} - (\text{CH}_2)_4 - $	~ 2	138±5	TL too weak for analysis	

TABLE 1 (Continued)

COMPOUND, SOURCE AND STRUCTURE OR SIDE GROUP	TL INTENSITY IN mμ AMP	T _p °K	E ev	γ min ⁻¹
Phenylglycine (NBCo) 	< 1	-	-	-
Tyramine-mono HCl (CCBR)	18 15	109 131	.08±.015	9.10 ³
	~ 2 ~ 3	166±5 194±5	TL too weak for analysis TL too weak for analysis	
D-Dihydroxyphenylalanine (NBCo) 	10	~ 102	TL too weak for analysis	
3-Hydroxytyramine.HCl (NBCo) 	~ 2	122±5	TL too weak for analysis	
Indole-3-Acetic Acid (NBCo) 	~ 2 ~ 14	116 155±5	TL too weak for analysis This glow curve looks like the sum of several unresolved peaks.	
Tryptamine.HCl (NBCo) 	100	113	.13	3.10 ⁴

CCBR - California Corporation for Biochemical Research

NBCo - Nutritional Biochemicals Corporation

irradiation with ultraviolet light at 77° K. A semilogarithmic plot of this luminescence shows that it can be resolved into the sum of two exponential decays, one with a half life of 3.1 seconds, the other with a half life of 92 seconds. This analysis is shown in Fig. 18. Figure 19 shows the initial curve analysis of the first peak of the L-phenylalanine glow curve. The points seem to form a tilted S-shaped curve rather than the straight line drawn through them. However the deviation from a straight line is everywhere less than the error due to the absolute uncertainty of the temperature ($\pm 3^{\circ}$ K) and may be due to systematic errors of the temperature measuring equipment. The error bars in Fig. 19 are derived from the absolute uncertainty of the temperature measurements. The overlap of the two peaks makes the analysis of the second peak for values of E and γ quite uncertain.

Additional evidence regarding the association of monomolecular kinetics with amino acid glow curves comes from the comparison of the theoretical expression (2-26) with the experimental data. The Burroughs Algebraic Compiler at the Stanford Computation Center was used to obtain numerical values for this expression. In doing so, experimental values of E and γ , and temperature as a function of time, $T(t)$, were used. The computer was programed to evaluate (2-26) over a time span covering the glow curve, in increments of .02 minutes. The actual program used, in the language of the computer, is given in Appendix II.

For the case of L-phenylalanine, the computed curves are compared to the experimental data from CCBRL-phenylalanine. Analysis of the first peak of a typical glow curve yielded the values $E = 0.095$ ev , $\gamma = 3.81 \cdot 10^4 \text{ min}^{-1}$. The theoretical curves obtained using these and certain other values of E , γ are shown in Fig. 20; the experimental curve is also shown for comparison.

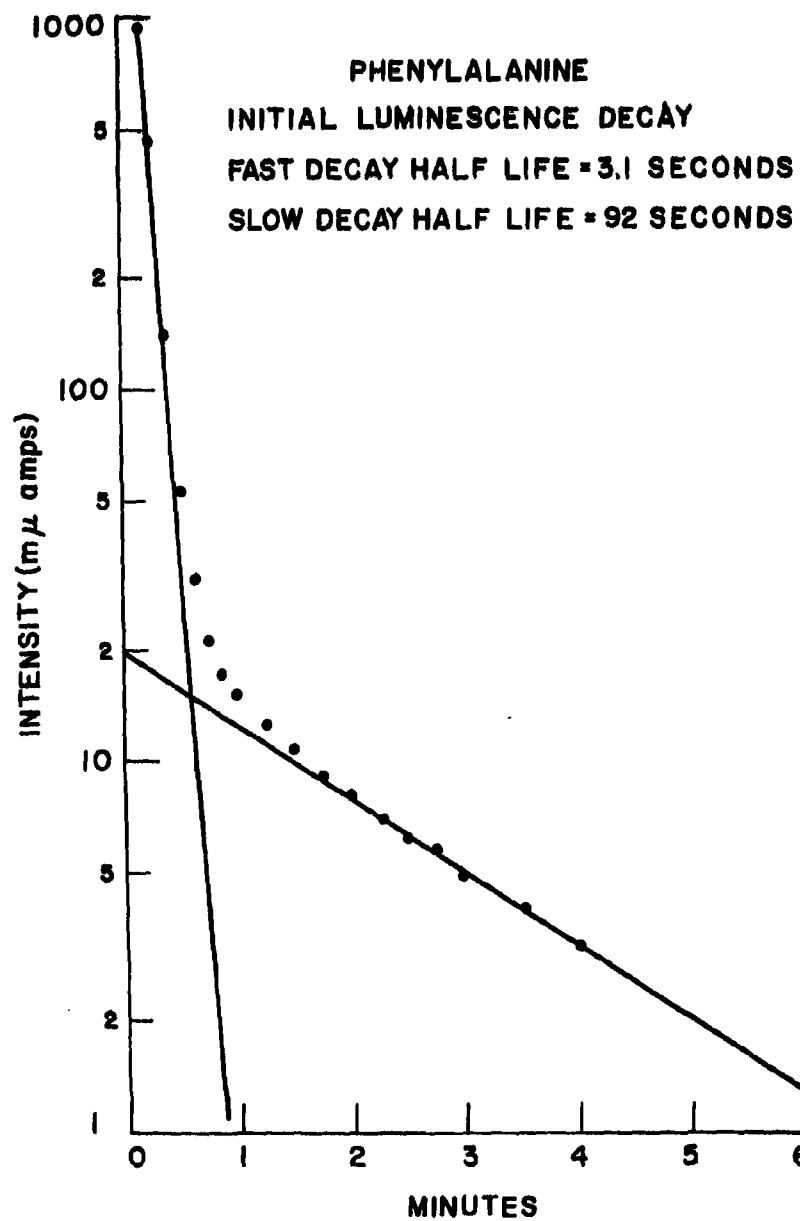


FIG. 18--Semilogarithmic plot of the phosphorescence decay from uv irradiated L-phenylalanine at 77° K.

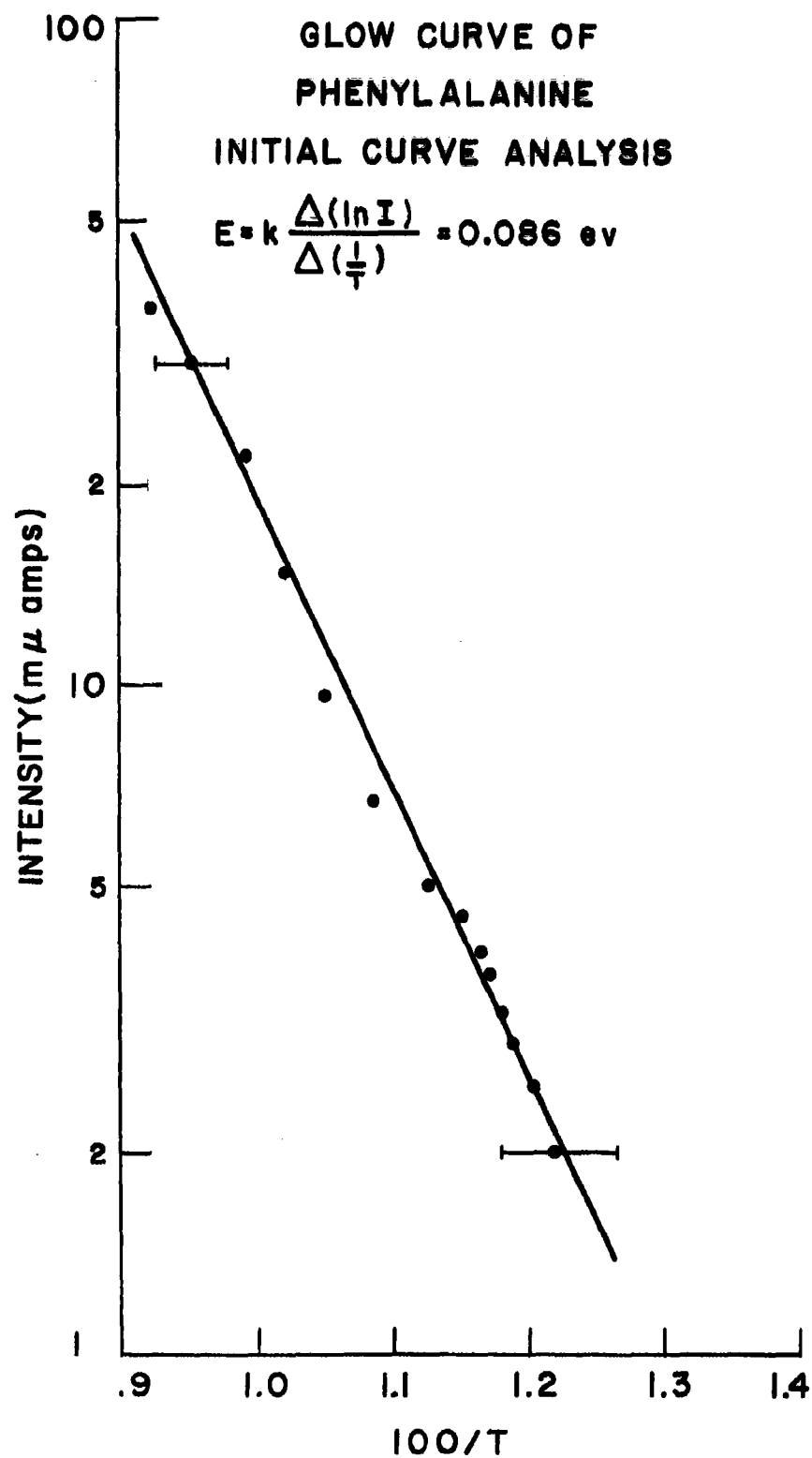


FIG. 19--Semilogarithmic plot of intensity versus 100/T for the initial part of the phenylalanine glow curve.

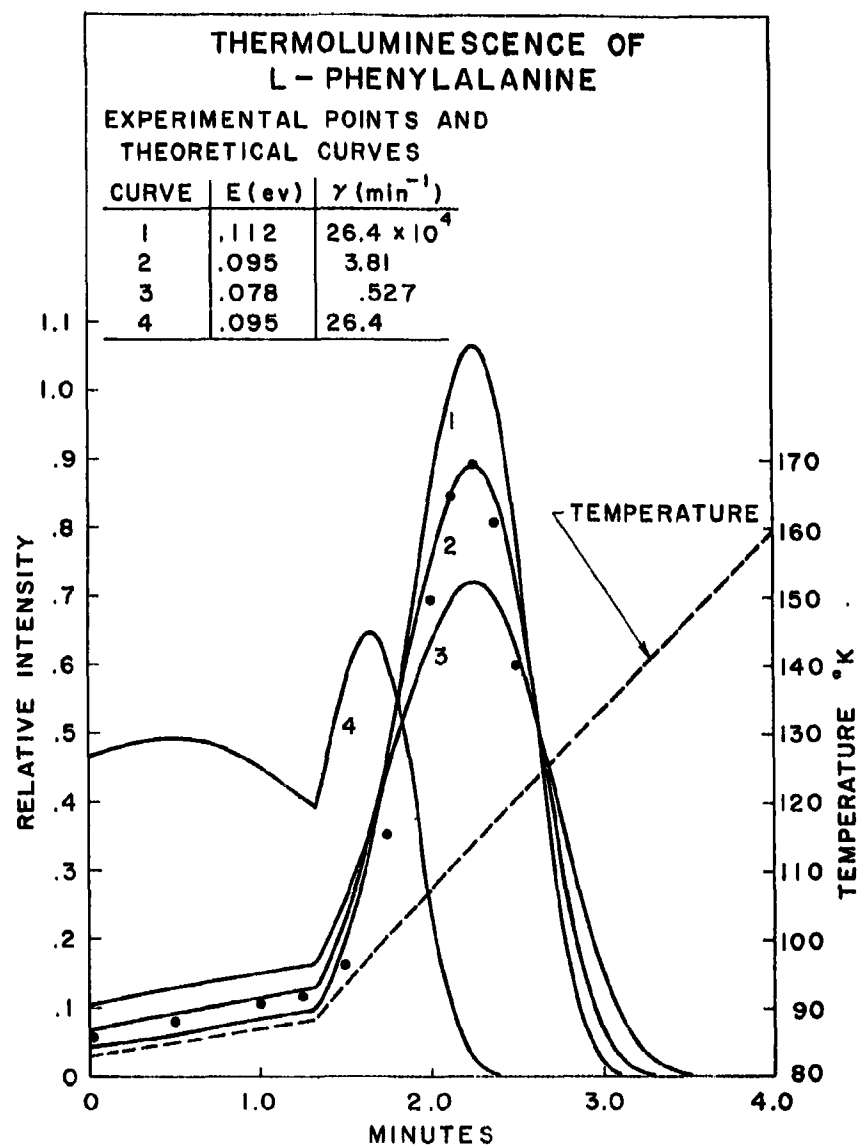


FIG. 20--A comparison of experimental points and theoretical curves computed using the parameters listed. The experimental points - shown as dots - are from the low temperature peak of an L-phenylalanine glow curve. The solid lines are plots of Eq. (2-26).

Theoretical and experimental glow curves of L-tyrosine (CCBR) are shown in Fig. 21. Using the temperature and intensity curves of a typical experiment, we obtained the values $E = .158 \text{ ev}$, $\gamma = 8.11 \cdot 10^6 \text{ min}^{-1}$. These values and the temperature curve were then used in obtaining a numerical plot of Eq. (2-26) with $gn(0)$ set equal to 1. Numerical plots were also made using the values $E = .181 \text{ ev}$, $\gamma = 81.6 \cdot 10^6 \text{ min}^{-1}$ and $E = .129 \text{ ev}$, $\gamma = .453 \cdot 10^6 \text{ min}^{-1}$. The values of γ were chosen so that the curves peaked at the experimentally observed temperature. There is a rather conspicuous disagreement between experiment and theory on the high temperature side of the glow curve in that the measured thermoluminescence persists somewhat longer than theory would predict. Possible explanations are (1) the frequency factor γ is not a constant with respect to temperature and (2) there is a second weaker thermoluminescence peak which cannot be resolved but which has a peak temperature greater than 125° K .

Another experiment concerning the pertinence of the monomolecular model is the following. A small amount of L-phenylalanine was dissolved in distilled water and one ml of the solution frozen to 77° K on the sample plate. This frozen solution produced weak thermoluminescence after being irradiated with ultraviolet; a one ml sample of frozen distilled water did not. The thermoluminescence observed from the frozen solution corresponds roughly to the low temperature peak of powdered L-phenylalanine. In addition, samples of L-phenylalanine, D-phenylalanine and L-tyrosine have been freeze dried from distilled water solution and found to exhibit thermoluminescence. In fact, samples of D-phenylalanine do not show thermoluminescence until freeze dried. These experiments show that thermoluminescence still occurs when the materials are in a

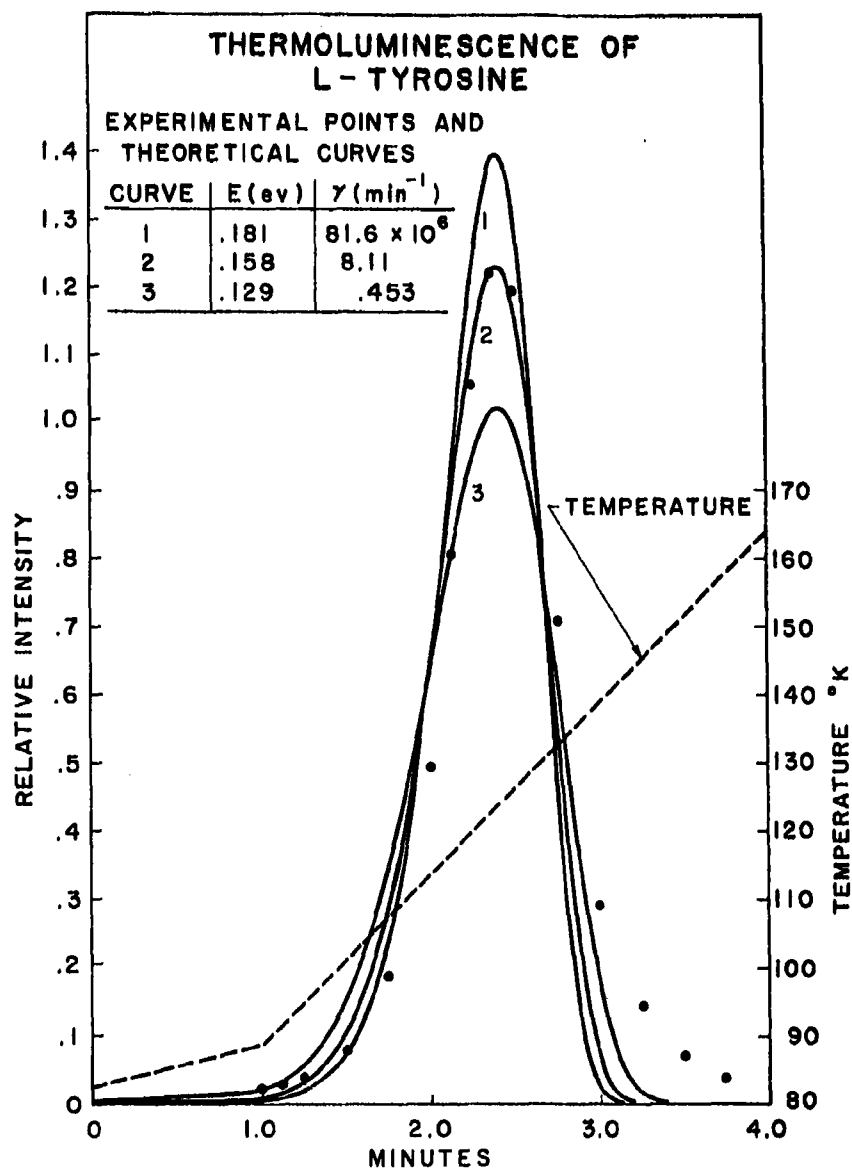


FIG. 21--A comparison of experimental points from an L-tyrosine glow curve with theoretical glow curves computed using the parameters listed.

dissolved or amorphous state and thus that crystalline structure is not essential.

Knowledge of the spectrum of the thermoluminescence would also be helpful in understanding the physics of the process. Unfortunately the intensity is too weak to permit the luminescence to be passed through a monochromator and still be detected. A crude spectrum has been obtained in the following way.

It was first determined that repeated cooling, ultraviolet irradiation and warming of the sample did not diminish the thermoluminescence response. Then a series of experiments was performed with the same sample, each time covered with a different Corning sharp cut glass filter. Comparison of the intensity measured in these experiments permits a rough estimate of percentage of luminescence with wavelength greater than certain values. The results of these measurements are given in Table 2. The filters used have CS numbers 3-70, 3-72, 3-74 and 3-75.

TABLE 2

<u>Compound</u> (all CCBR)	<u>Percentage of Thermoluminescence with Wavelength</u>				
	<u>>6000 Å</u>	<u>>5030 Å</u>	<u>>4500 Å</u>	<u>>4080 Å</u>	<u>>3980 Å</u>
L-tyrosine	0	16	37	73	95
L-phenylalanine (1st peak)	0	16	40	75	85
L-phenylalanine (2nd peak)	0	16	46	80	90
Egg Albumin (Protein)		10	50		95

The figures given in this table are estimated to be within 20% of the correct values.

Dose response measurements have been made on L-tyrosine and L-phenylalanine by irradiating the samples for varying lengths of time and comparing the relative amplitudes of resulting thermoluminescence. For both compounds, a dose of $2 \cdot 10^7$ ergs (30 seconds illumination) was sufficient to produce the maximum level of response, while a dose of $6 \cdot 10^6$ ergs produced half the maximum level. The quantum yield of the thermoluminescence produced by these materials is roughly one part in 10^8 .

Next to be considered is the nature of the metastable excited states. The three hypotheses proposed in Chapter II were (1) trapping at an ionic portion of a molecule, (2) a frozen isomerization, and (3) a photo induced charge-transfer complex involving a metal ion. The evidence which is helpful in deciding which of these is correct is (a) only about one molecule in 10^9 develops this metastable state, (b) the same compound from different biochemical suppliers shows different thermoluminescence responses, (c) the naturally occurring L isomer of phenylalanine develops thermoluminescence, while the artificially synthesized D isomer does not. These three pieces of evidence seem most consistent with the third hypothesis. It appears that trace amounts of some metal ion come through the isolation procedures with the naturally occurring amino acids and proteins, but do not occur in the laboratory synthesized D isomer of phenylalanine. The actual presence of trace amounts of metal ions has been determined in two ways. Distilled water solutions of L-tyrosine and L-phenylalanine were shaken with a solution of the chelating agent 8-quinolinol in CCl_4 . After a few hours, a distinct color appeared indicating the presence of copper or iron ions or both.* Wide sweep

*I am indebted to L. Taskovich for this technique.

EPR measurements of tyrosine and phenylalanine samples revealed the presence of paramagnetic ions, their abundance being a few parts per million.* Further, tyrosine was dissolved, filtered and recrystallized from water solution. The thermoluminescence response of the purified material was about 15% of the untreated tyrosine. The filtrate was freeze dried and found also to exhibit thermoluminescence. It appears that some substance which was present in the untreated sample was partially removed by the recrystallization, going at least in part into the filtrate. This result suggested the following experiment. It seemed likely that if an ion, present in trace amounts, were necessary for thermoluminescence, adding an abundance of this ion would greatly increase the intensity of the response. Table 3 summarizes the results of adding one part of the salts listed to a water solution of ten parts of (CCBR) L-phenylalanine, freeze drying the mixture and examining for thermoluminescence. Of the ten salts tried, only two enhance the response, only one appreciably. Copper and iron salts quench the response entirely. Thus copper and iron are removed from suspicion as the unknown complexed quantity and calcium is introduced as the only likely agent of the materials tested. Further work and more sophisticated chemistry are needed before the amino acid-metal ion complex hypothesis can be accepted with certainty.

Polymers of amino acids have been found to exhibit thermoluminescence although the results are not what one would predict from the monomer case. Poly L-tyrosine, for example, shows a weak response and poly L-phenylalanine a stronger response but only one peak. (See Fig. 22.) These results

*These measurements were kindly performed by Dr. J. Maling.

TABLE 3

<u>Salt Added</u>	<u>Result</u>
NaCl	Intensity of first peak normal Intensity of second peak reduced to half value
MgSO ₄	Intensity of first peak normal Intensity of second peak reduced to about half value
MnCl ₂	Intensity of both peaks reduced to about one-third normal value
CoCl ₂	Intensity reduced to about one-fourth normal value
Na ₂ MoO ₄ ·2H ₂ O	Intensity of both peaks reduced to about one-third normal value
ZnSO ₄	Intensity of first peak enhanced by about 20% Intensity of second peak about half normal value
FeCl ₃	This salt completely quenches both peaks
CaCl ₂	Intensity of first peak increased by a factor of 3 Second peak about one-fourth normal value
CuCl ₂ ·2H ₂ O	Both peaks completely quenched
CuCl	Both peaks completely quenched

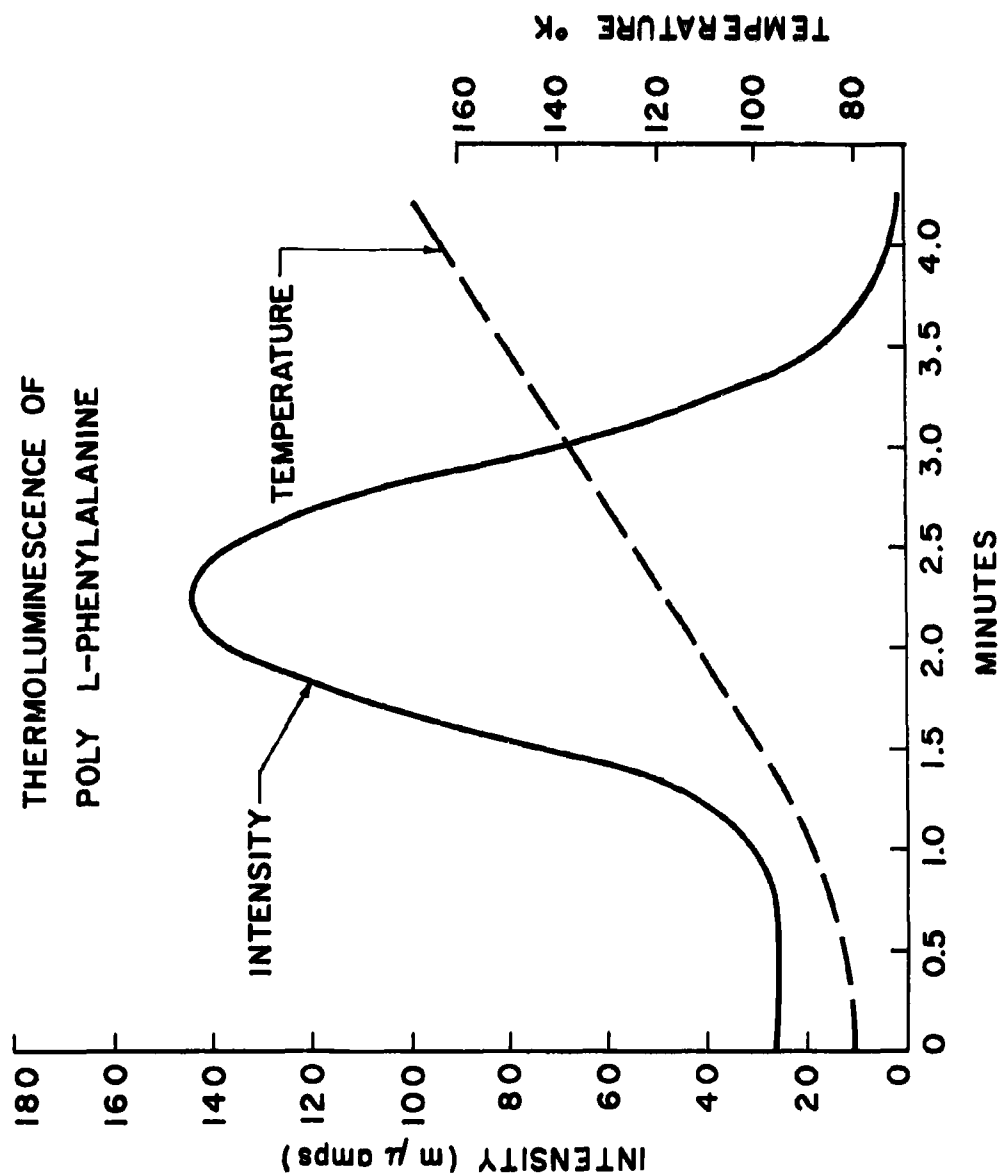


FIG. 22--Glow curve of uv irradiated poly L-phenylalanine.
The peak temperature is 114° K.

and the results of experiments on di- and tripeptides and on proteins are summarized in Table 4.

The iron-free proteins which were examined showed a very long-lived luminescence at 80° K. The decay is complex but can, in the case of egg albumin, be resolved as shown in Fig. 24. The lifetime of this luminescence is very temperature dependent. Had lower temperatures been available, this luminescence could have been frozen in, with much longer lifetimes. Because the luminescence leaks out at 80° K, the intensity of the peak varies considerably. The glow curve of trypsin was found to be more reproducible; it is shown in Fig. 23.

Note that this curve, in contrast to those of Figs. 15 and 17 has a steeper slope on the ascending than the descending side. This contrast is consistent with a change from monomolecular to polymeric kinetics. Figure 25 shows graphs made of (2-26) and (2-65) using the same values of E , γ and the same dependence of T upon t . Both curves were normalized by setting the integral of the intensity equal to 1. The monomer curve has its steepest slope on the descending side, while the $L = 4$ polymer curve is nearly symmetric but is slightly less steep on the descending side. This asymmetry will be pronounced for larger L .

Thus we conclude that the polymer glow curves are consistent with the charge migration hypothesis and that the process is an intramolecular one. The absence of thermoluminescence from ferritin and cytochrome C and also from a lyophilized mixture of egg albumin and ferris chloride indicates that iron somehow quenches the luminescence from polypeptides as well as from L-phenylalanine.

TABLE 4

<u>Compound</u>	<u>Results</u>
Glycyl L-Phenylalanine NBCo	One peak, intensity 8 mμ amp, $T_p = 108^\circ \text{K}$
Glycyl L-Tyrosine NBCo	One peak, intensity 12 mμ amp, $T_p = 136^\circ \text{K}$, a shoulder on low temperature at $T = 104^\circ \text{K}$
DL Leucyl-Glycyl DL Phenylalanine NBCo	One peak, intensity 7 mμ amp, $T_p = 116^\circ \text{K}$ with shoulders on both high and low temperature sides
Poly L-Tyrosine Yeda	One peak, intensity 10 mμ amp, long tail on high temperature side
Poly L-Phenylalanine	See Fig. 22
Trypsin CCBR	See Fig. 23
Egg Albumin: 10 mg in 1 ml distilled H_2O CCBR	One peak, intensity about 50 mμ amp, but dependent upon length of time after uv irradiation - $T_p = 120^\circ \text{K}$
Chymotrypsin CCBR	Sample shows long-lived decay and glow curve much like that of Trypsin
Cytochrome C CCBR	No thermoluminescence or long-lived initial glow
Ferritin CCBR	No thermoluminescence or long-lived initial glow

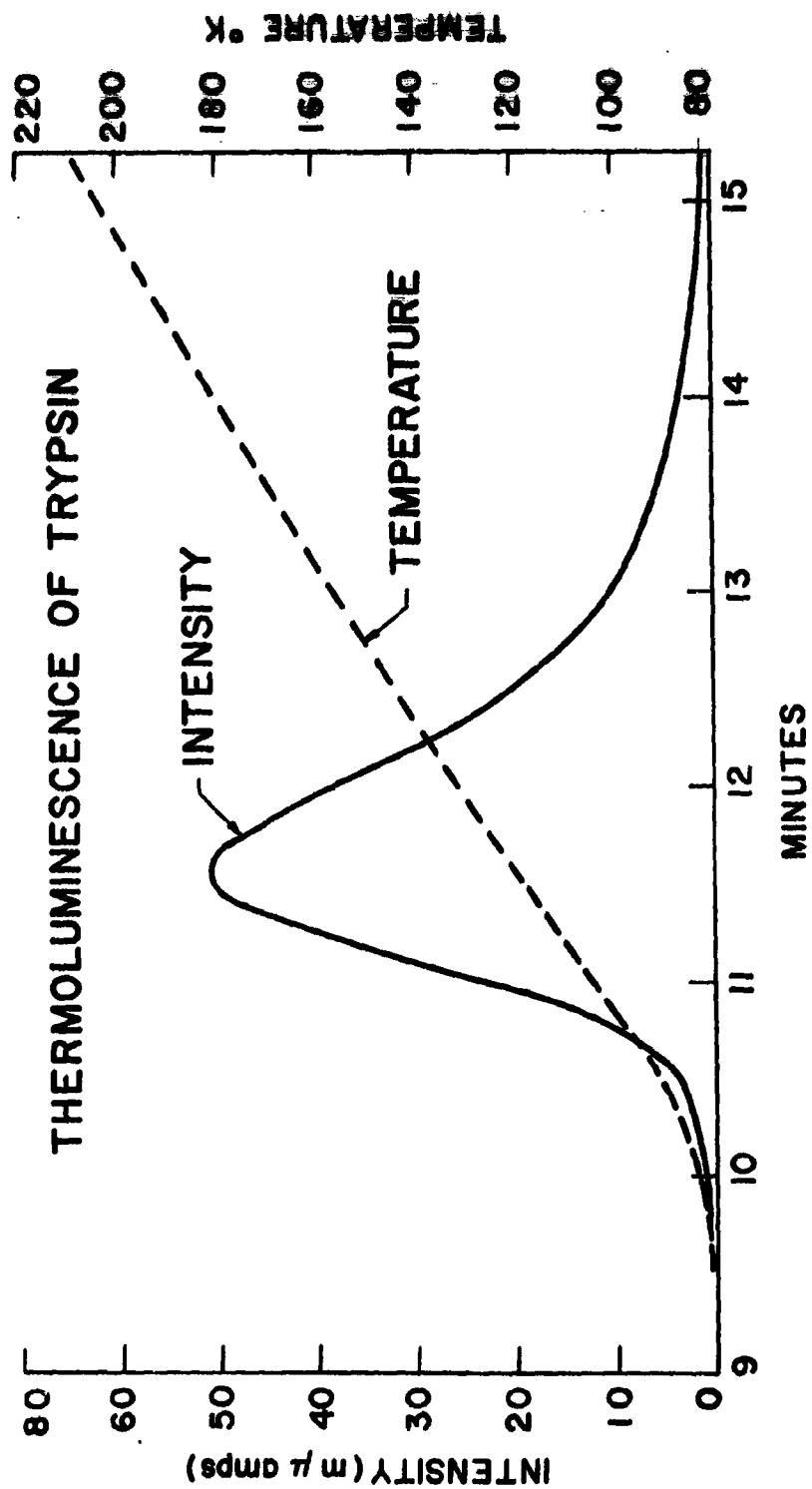


FIG. 23--Glow curve of uv irradiated trypsin.

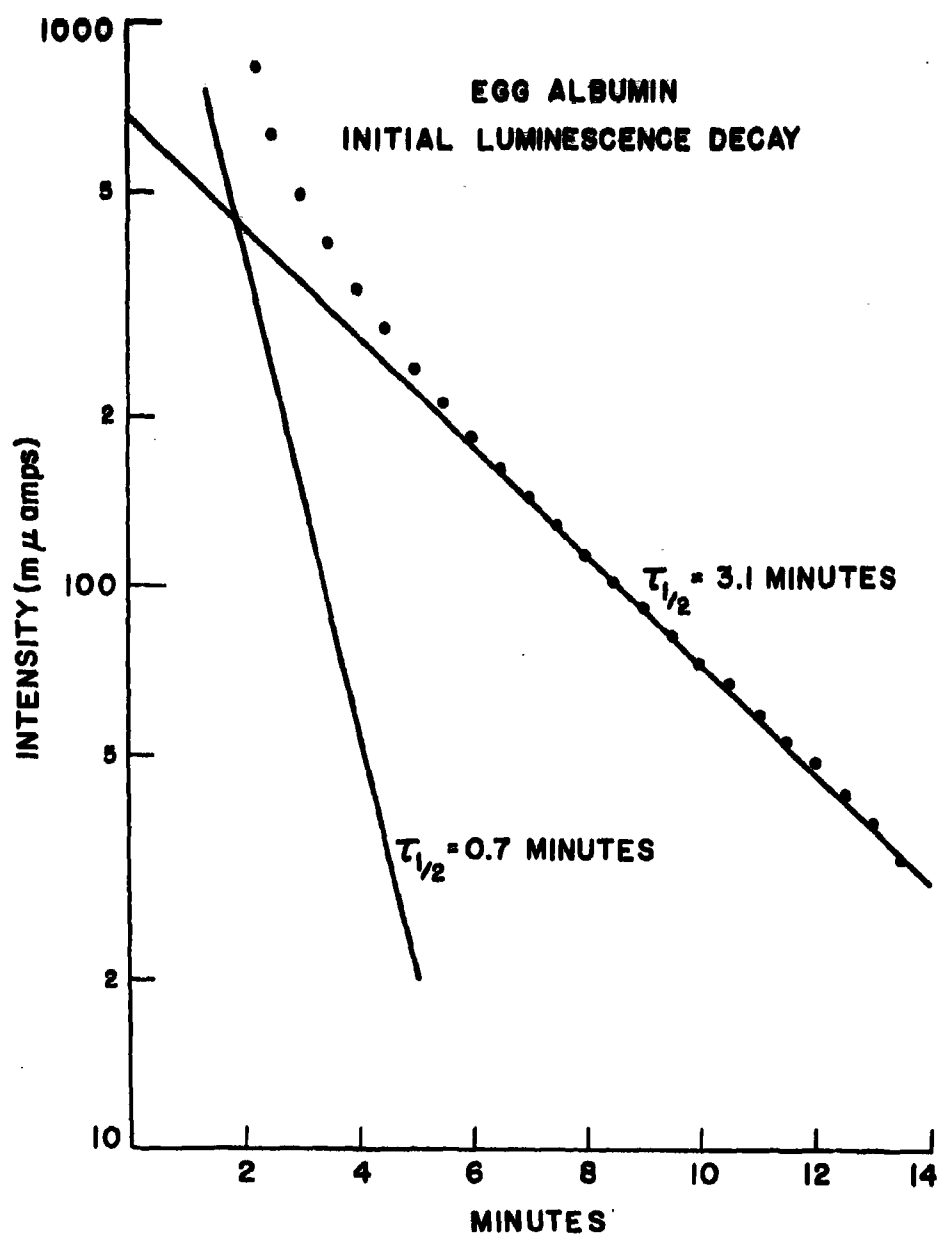


FIG. 24--Semilogarithmic plot of the decay of phosphorescence from uv irradiated egg albumin at 77° K .

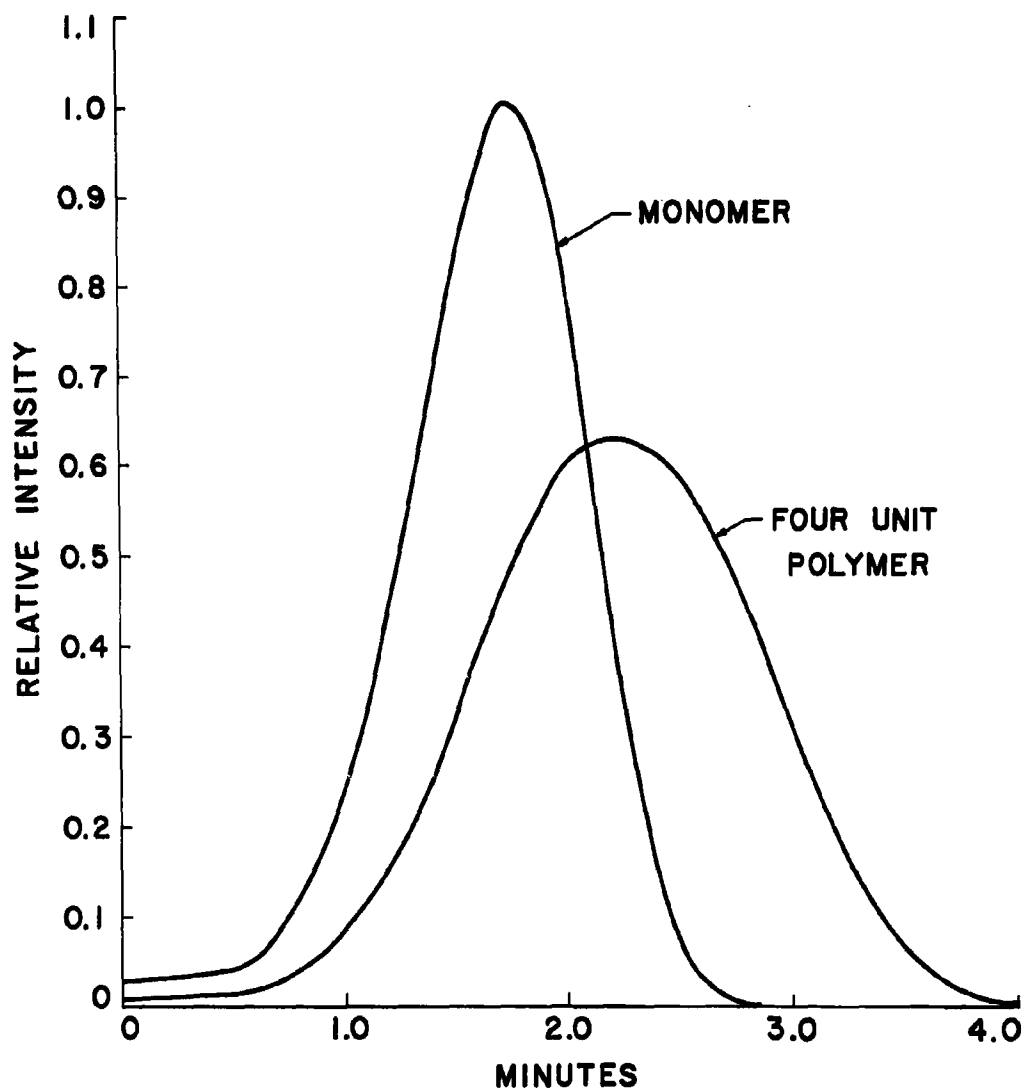


FIG. 25--Comparison of theoretical glow curves from a monomer and a four-unit polymer. The same values of E , γ and $T(t)$ were used in computing these curves.

CHAPTER IV
RESULTS AND INTERPRETATION OF ELECTRON
PARAMAGNETIC RESONANCE EXPERIMENTS

When polycrystalline samples of amino acids, polypeptides or proteins are irradiated with ultraviolet light at 80° K, they develop paramagnetism which can be measured by means of an EPR (electron paramagnetic resonance) spectrometer. This paramagnetism can be interpreted as arising from free radicals or trapped electrons or ions - products of the absorption of the ultraviolet light by the molecules of the sample.

The physics of EPR absorption by unpaired spins is fully discussed in the literature.¹ For the studies reported here, one may describe the phenomenon in terms of a dilute ensemble of unpaired electrons in the material under investigation. These electrons interact (1) with an externally applied magnetic field, (2) with a rapidly varying magnetic field in the microwave cavity containing the material, (3) with the electrostatic crystal field due to surrounding atoms or molecules, (4) with the magnetic moments of neighboring atomic nuclei.

The first two interactions may be represented by the spin Hamiltonian

$$\mathcal{H} = g\beta H_0 S_z + g\beta 2H_1 \cos(\omega t) S_x \quad (4-1)$$

where g is the spectroscopic splitting factor

β is the Bohr magneton

H_0 is the externally applied magnetic field which defines the z-axis

S_z is the z-component of the spin operator

¹G. E. Pake, Paramagnetic Resonance (Benjamin, New York, 1962).

$2H_1 \cos(\omega t)$ is the microwave magnetic field

S_x is the x-component of the spin operator.

The second term in (4-1) serves as a perturbation which causes transitions between eigenstates, $\langle S_z \rangle = \pm \frac{1}{2}$, of the first term. The probability of these transitions is proportional to

$$|M|^2 = \left(\frac{g\beta H_1}{\hbar} \right)^2 \frac{\sin^2(\Delta/2)t}{\Delta^2} \quad (4-2)$$

where

$$\Delta = \frac{g\beta H_0}{\hbar} - \omega .$$

There are two effects which cause the smearing out of the resonance condition,

$$g\beta H_0 = \hbar \omega . \quad (4-3)$$

(1) Because of the electron-crystal field interaction, the g-factor is slightly dependent upon the orientation of the crystal field relative to H_0 . In polycrystalline samples where all orientations occur, g has a range of values, with $\Delta g/g \approx 10^{-3}$ in amino acid samples.

(2) There are local variations in H_0 within the sample. These two effects may be taken into account by introducing a density function $f(\omega)$ for the resonance frequency. Then one can show that the transition rate between eigenstates of S_z is

$$V = \left(\frac{g\beta H_1}{\hbar} \right)^2 \frac{\pi}{2} f(\omega) . \quad (4-4)$$

Experimentally, the resonance is detected when the transitions result in the sample absorbing power from the microwave field. If N is the number of unpaired spins in the sample, and W is the spontaneous

spin-flip probability, the power absorbed is

$$P(\omega) = \frac{\hbar \omega V N \tanh(g\beta H_0 / 2kT)}{1 + 2T_1 \nu}, \quad (4-5)$$

where

$$T_1 = \frac{1}{W[1 + \exp(g\beta H_0 / kT)]}.$$

The interaction between the spin of the unpaired electron and the moments of neighboring atomic nuclei is called the hyperfine interaction. It can be treated by adding the term

$$\mathcal{H}_{hf} = \sum_{\text{Nuclei}} A_i \mathbf{I}_i \cdot \mathbf{S} \quad (4-6)$$

to (4-1). In the representation in which the first term of (4-1) is diagonal, (4-6) combines with this term to give

$$\langle \mathcal{H} \rangle \cong g\beta H_0 m + \sum_{\text{Nuclei}} A_i M_i m. \quad (4-7)$$

Here, M_i is the magnetic quantum number of the i th nucleus, m that of the electron and A_i is the strength of the interaction. Equation (4-7) may be rewritten as

$$\langle \mathcal{H} \rangle \cong g\beta \left(H_0 + \sum_i \frac{A_i}{g\beta} M_i \right) m \quad (4-8)$$

showing that this interaction produces a shift in the resonance condition. Consider this special case where an electron interacts equally with two hydrogen nuclei. The sum in (4-8) can take on three values depending upon the orientation of the two protons' magnetic moments relative to \vec{H}_0 . The three possible orientations are: (1) both moments parallel to \vec{H}_0 ; (2) both moments antiparallel to \vec{H}_0 ; (3) one moment parallel

and one moment antiparallel. Thus, electrons interacting equally with two protons will undergo spin-flip transitions when $\omega = \bar{g}\beta H_0$ (case 3) and when $\omega = \bar{g}\beta[H_0 \pm (2A/g\beta)]$ (cases 1 and 2). The resulting three-line absorption pattern is believed to account for part of the observed absorption by ultraviolet irradiated glycine. (See Fig. 26.)

Our EPR studies have been directed toward the following questions.

- (1) Which amino acids, related molecules and proteins develop paramagnetism when irradiated with ultraviolet light at 77°K ?
- (2) What is the location of the unpaired electron which is presumably responsible for the resonance?
- (3) Are unpaired electrons producing the resonance also involved in the production of thermoluminescence?

The following apparatus and materials were used in the experimental work: (1) A Varian Associates EPR spectrometer and six-inch electromagnet form the basic instrument. (2) A quartz liquid nitrogen Dewar designed to fit inside the microwave cavity is used to keep the sample at 77°K during ultraviolet irradiation and EPR absorption measurements. Quartz tubes 3 mm or 4 mm in diameter contain the sample materials. (3) A Hanovia type 30600 140 watt ultraviolet lamp is used for irradiation. The light passes through a Corning Vycor glass filter before reaching the Dewar. This filter absorbs light of wavelength shorter than 2300 \AA . (4) Biochemicals used are obtained from CCBP and NBCo and are the purest available from those companies.

The experimental procedure has been to seal the compounds as they are supplied by the vendor inside clean quartz tubes, to cool the materials by immersing the tubes in liquid nitrogen, to irradiate the tubes while they are immersed in liquid N_2 , to measure the EPR absorption of the

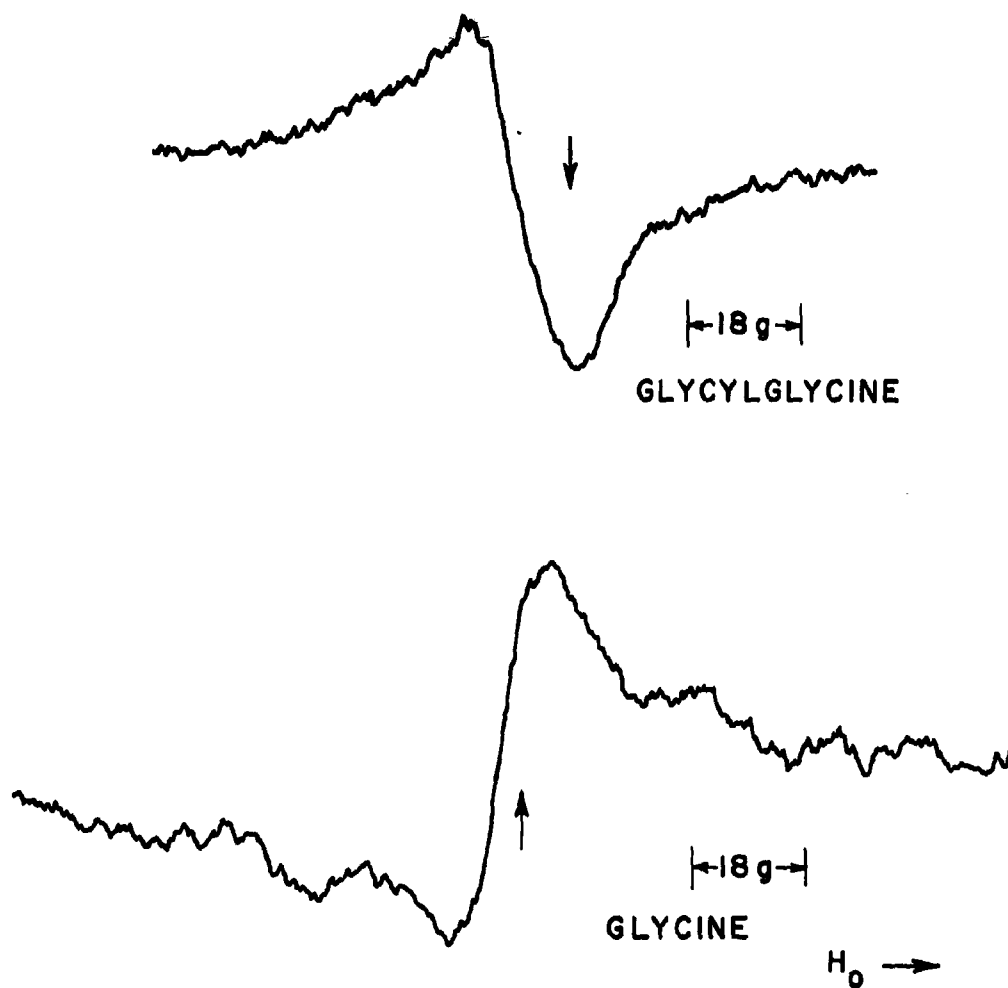
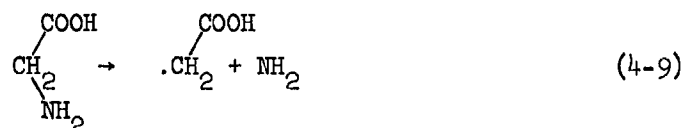


FIG. 26--First derivative traces of paramagnetic resonance absorption in glycyglycine and glycine measured as a function of magnetic field H . The amplitude of the 100 KC modulation of H_0 was 1.5 gauss peak to peak with glycyglycine, 2.5 gauss with glycine. Maximum value of microwave magnetic field at sample was $H_1 = 0.1$ gauss in each case. These compounds were irradiated in the dry state with ultraviolet light and the resonance absorption was measured afterward without changing the sample temperature from 77° K. Position of the DPPH absorption ($g = 2.0036$) is indicated by an arrow.

sample at 77° K and again at room temperature. The apparatus produces a chart recording of the first derivative of the absorption.

A number of amino acids develop only a weak absorption when treated in this way. Glycine is a typical example of this class of amino acids. Its first derivative trace is shown in Fig. 26. Although this signal is weak, as indicated by the relative noise level, the shoulders indicating a three-line absorption are real and reproducible as has been confirmed by Simmonds.² This three-line component of the signal may be due to a free radical intermediate of photo-induced deamination. This reaction is common to most amino acids^{3,4} and would be responsible for part of the EPR signal developed by them. In the case of glycine this reaction may proceed in part as shown in (4-9).



where the dot at the α -carbon represents an unpaired electron.

The signal produced in glycylglycine which shows no triplet character indicates that some other free radical must also be produced. Without doing studies on single crystals, as Gordy⁵ has done using x-rays, it is not possible to form an opinion about the structure of this radical. Other amino acids which develop this weak single absorption line are L-glutamic acid, L-cystine, L-histidine, L-tryptophan and L-phenylalanine.

²J. A. Simmonds, private communication.

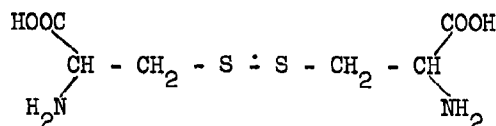
³J. Greenstein and M. Winitz, Chemistry of the Amino Acids (John Wiley and Sons, New York, 1960).

⁴A. Horsfield, J. Morton, D. Whiffin, Trans. Faraday Soc. 57, 1657 (1961).

⁵M. Katayama and W. Gordy, J. Chem. Phys. 35, 117 (1961).

In each case, warming the sample to room temperature reduced the EPR signal intensity by roughly a factor of five.

Cysteine, when treated as described, developed a strong five-line absorption. This is shown in Fig. 27. The shape of this trace is consistent with the hypothesis that the unpaired electron interacts about equally with four protons, suggesting that irradiation induces dimerization with an unpaired electron at the disulfide bond, as indicated in the sketch below.



It is further observed that when the sample is warmed to room temperature, the absorption changes from a five-line to a three-line pattern with about 20% of the low temperature intensity. This may be the result of the breaking apart of the free radical dimer and the formation of a cysteine free radical with the unpaired electron at the S - CH₂ region. Cystine, the disulfide bond dimer of cysteine develops only the weak single-line absorption shown at the top of Fig. 27, when treated as described. EPR studies of cystine following x-ray irradiation⁶ have shown that the sulfur atom is able to accept an unpaired electron even when this atom is involved in a disulfide bond. The resonance observed looks much like the room-temperature trace of cysteine resonance in Fig. 27. The dimer cystine thus seems rather impervious to ultraviolet light, though not to x-rays, in marked contrast to the monomer cysteine.

⁶J. Henriksen in Free Radicals in Biological Systems (edited by M. S. Blois, et al., Academic Press, New York, 1961).

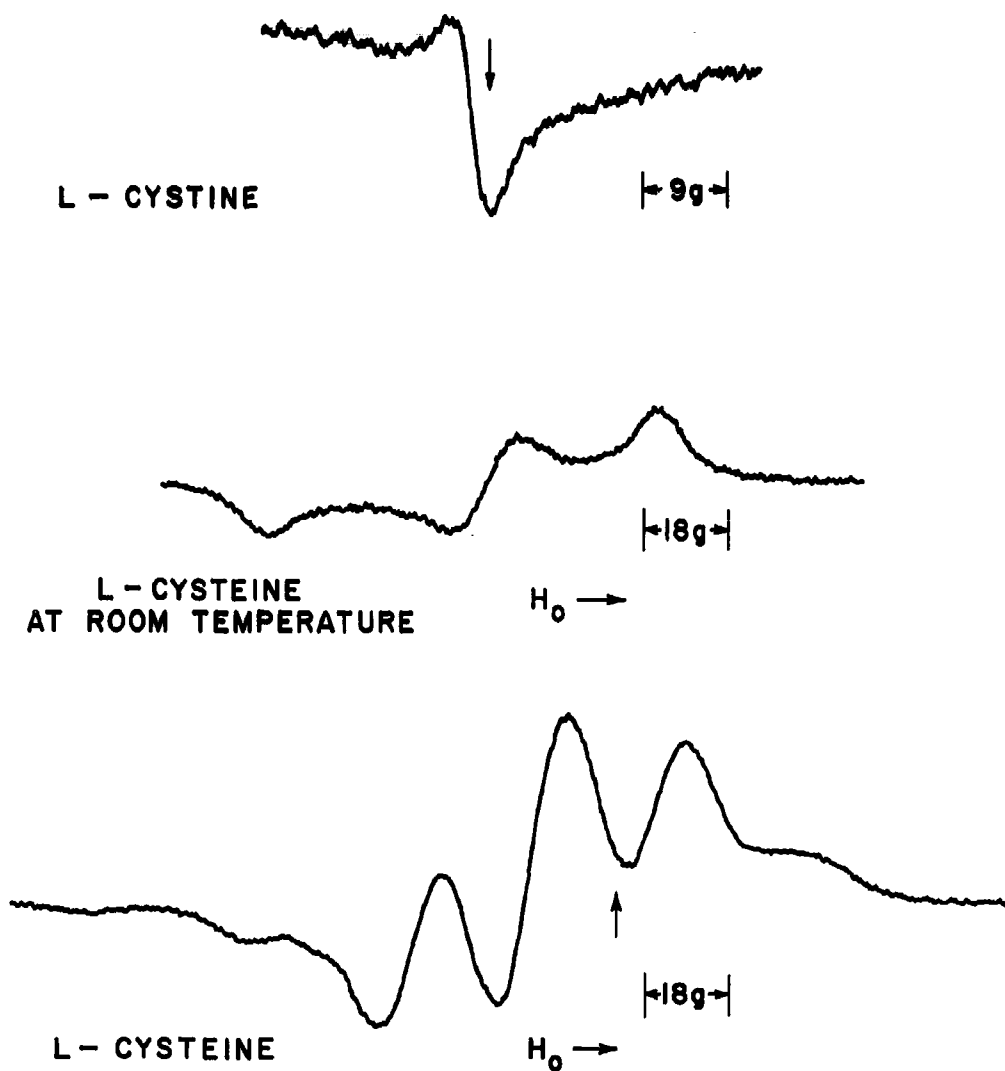


FIG. 27--First derivative traces of paramagnetic absorption in L-cystine and L-cysteine. Measurements on L-cystine were made using 2.5 gauss peak-to-peak 100 KC modulation and an H_1 amplitude of 0.15 gauss. For cysteine, the 100 KC modulation amplitude was 0.15 gauss peak-to-peak at both temperatures. H_1 amplitudes used were 0.07 gauss at 77° K, 0.10 gauss at room temperature. In each case the compounds were ultraviolet irradiated in polycrystalline form at 77° K.

Although glutamic acid and glycine do not develop a strong signal, their presence with cysteine in the tripeptide glutathione causes the EPR absorption developed by reduced glutathione to be much different from the sum of the spectra of the constituents. See Fig. 28. This absorption seems to be the superposition of a strong single absorption line upon the cysteine absorption. When a mechanical mixture of cysteine, glycine and glutamic acid is irradiated with ultraviolet light, only the cysteine absorption is observed. It thus appears that the formation of peptide bonds makes available new sites for unpaired electron trapping or free radical formation.

The EPR absorption developed in a number of aromatic amino acids and related molecules has been measured. Two classes of results are observed. Those compounds which contain hydroxy groups on the ring develop a strong single absorption line. Examples are tyrosine, tyramine, dihydroxy-phenylalanine, and 3-hydroxy tyromine. On the other hand, those compounds such as L-phenylalanine, which lack an OH group on the ring show a weaker signal. The role played by the hydroxyl group is not clear. One possibility is that the OH group - being somewhat acidic when attached to a ring structure - is dissociated by the ultraviolet light giving off the proton, leaving an unpaired electron on the oxygen after the resulting rearrangement. A search was made for atomic hydrogen absorption in a sample of tyramine. It was not found. It may be that it could escape even at 77° K or that it was not formed by the ultraviolet irradiation.

Proteins develop EPR absorption signals which do not resemble those of any individual amino acid. Trypsin absorption is shown in Fig. 29. Egg albumin absorption at 77° K and at 300° K is shown in Fig. 30.

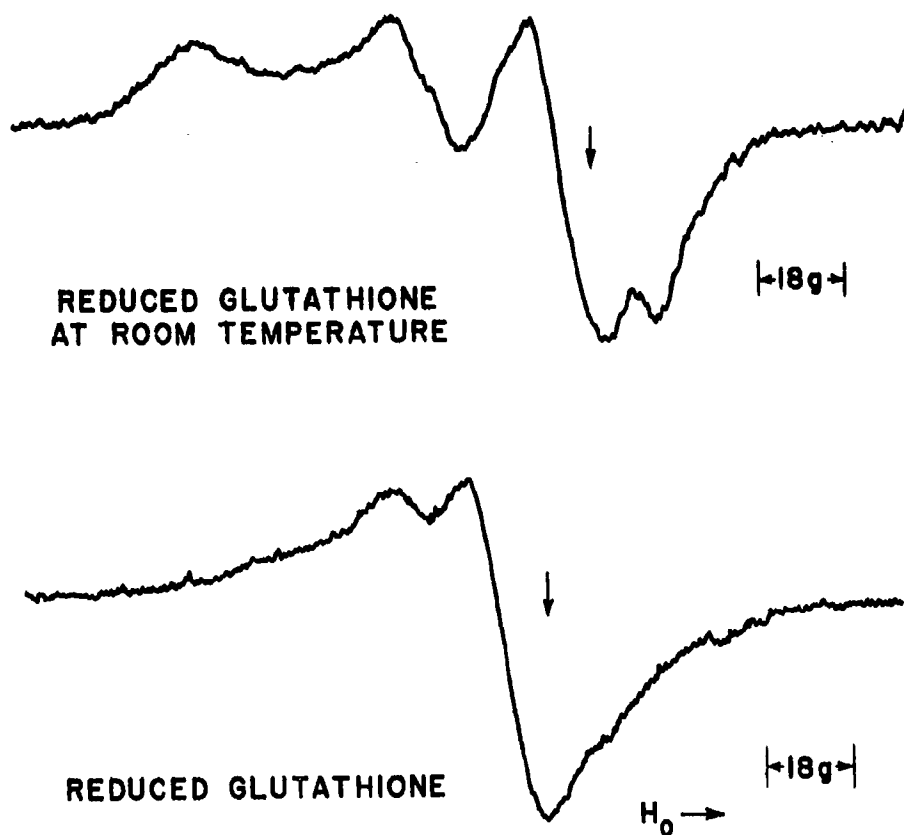
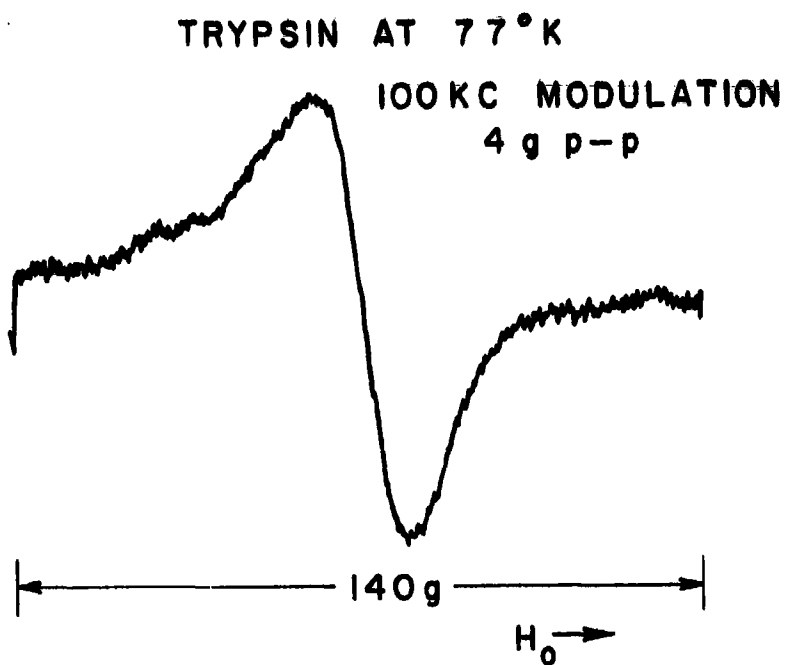


FIG. 28--First derivative traces of paramagnetic resonance absorption in reduced glutathione. This compound is a tripeptide composed of glutamic acid, glycine and cysteine. This compound, in the form of a dry powder, was placed in a tube and the tube was evacuated in an attempt to remove oxygen. The tube was then sealed and the compound was cooled to 77°K and irradiated with ultraviolet light. During the absorption measurements at 77°K , the 100 KC modulation amplitude was 0.6 gauss peak-to-peak and H_1 was approximately 0.15 gauss at room temperature, the 100 KC modulation was 2.0 gauss peak-to-peak, the H_1 field strength was unchanged.



TRYPSIN AT ROOM TEMPERATURE

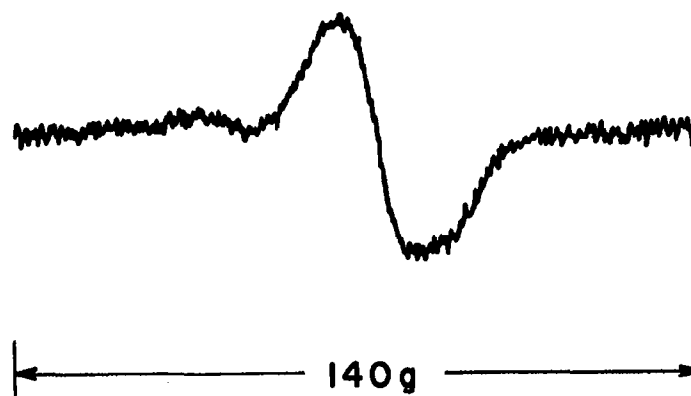
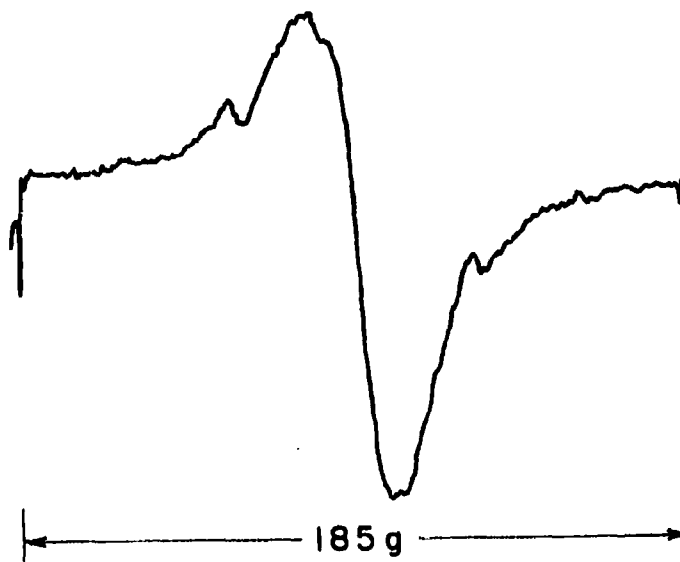


FIG. 29--First derivative trace of paramagnetic resonance absorption developed in polycrystalline trypsin after ultraviolet irradiation at 77° K. At 77° K the H_1 field was 0.07 gauss, at room temperature it was 0.1 gauss.

EGG ALBUMIN AT 77°K



EGG ALBUMIN AT ROOM TEMPERATURE

100 KC MODULATION
2.5 g p-p

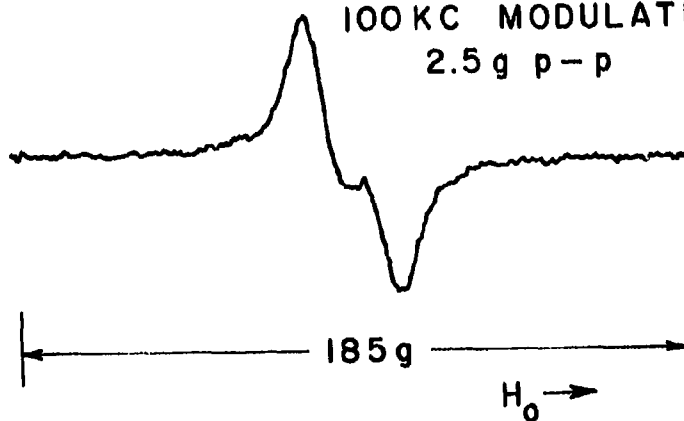


FIG. 30--First derivative traces of paramagnetic resonance absorption developed in egg albumin after ultraviolet irradiation at 77° K. The H_1 field was 0.1 gauss at both 77° K and room temperature.

Allen and Ingram⁷ find that egg albumin develops an EPR absorption when irradiated with 3650 Å at 77° K which disappears completely when the sample is warmed to room temperature. When they irradiated with 2537 Å ultraviolet light they produced an EPR signal which did not decrease when the sample was warmed to room temperature. Since the light used in our experiments contained both of the wavelengths used by these workers it may be that the signal shown at the top of Fig. 30 is the sum of the 3650 Å and 2537 Å response while the bottom trace is that of the 2537 Å response alone. Allen and Ingram interpret their results by assuming that molecules of egg albumin, in the presence of loosely bound water are able to act as band model semiconductors. They say "the most straightforward interpretation of the results on the egg albumin is that the electrons are being excited into the upper conduction band by the 3650 Å irradiation and some of these are then falling into low-lying traps formed by the presence of odd protons along the polypeptide chain system. On warming to room temperature, these trapped electrons are re-excited to the conduction band and then return to the ground state so that the resonance signal disappears." The results obtained by these authors could as well be interpreted in terms of the Markov process. The experimental evidence does not indicate which of these two hypothesis is closer to the truth. In fact it is not yet clear even in the case of the relatively simple anthracene molecular crystal whether charge-carrier motion should be described by the band model or the hopping model.

⁷B. T. Allen and D.J.E. Ingram, *Compte-rendu du 9^e Colloque Ampère*, p. 219, Pise, September 1960.

Bovine hemoglobin when irradiated at 77° K develops the EPR absorption shown in Fig. 31. The structure shown in this trace has not been interpreted. This absorption disappears below the weak preirradiation signal when the sample is warmed to room temperature. It is remarkable that the presence of iron causes the quenching of EPR signals at room temperatures and also of thermoluminescence from proteins.

Our EPR studies have shown that (1) ultraviolet irradiation at 77° K causes some absorption in many amino acids and probably all proteins. The ultraviolet induced deamination reaction (4-9) which results in an unpaired electron at the α -carbon may be responsible for at least part of the absorption observed in glycine, L-glutamic acid, L-cystine, L-histidine, L-tryptophan and L-phenylalanine. L-cysteine develops an absorption pattern which suggests that ultraviolet irradiation dimerizes this molecule at 77° K. Aromatic amino acids with OH groups attached to the ring develop a strong single-line absorption suggesting the OH group loses its proton when the molecule absorbs an ultraviolet photon. The tripeptide glutathione develops an absorption pattern which is more than the sum of the absorption patterns of the three constituents, glycine, L-glutamic acid and L-cysteine. All of the proteins examined, trypsin, egg albumin and bovine hemoglobin develop absorption after ultraviolet irradiation. There is some poorly resolved hyperfine structure which does not reveal the location of the unpaired electrons in the sample. (In polycrystalline material the smearing of the resonance condition (4-3) results in the smearing of the hyperfine structure. Conclusions based on interpretation of hyperfine structure must therefore be considered tentative.) (2) There is no evidence that the unpaired electrons responsible for EPR absorption are also involved in the

BOVINE HEMOGLOBIN AT 77°K

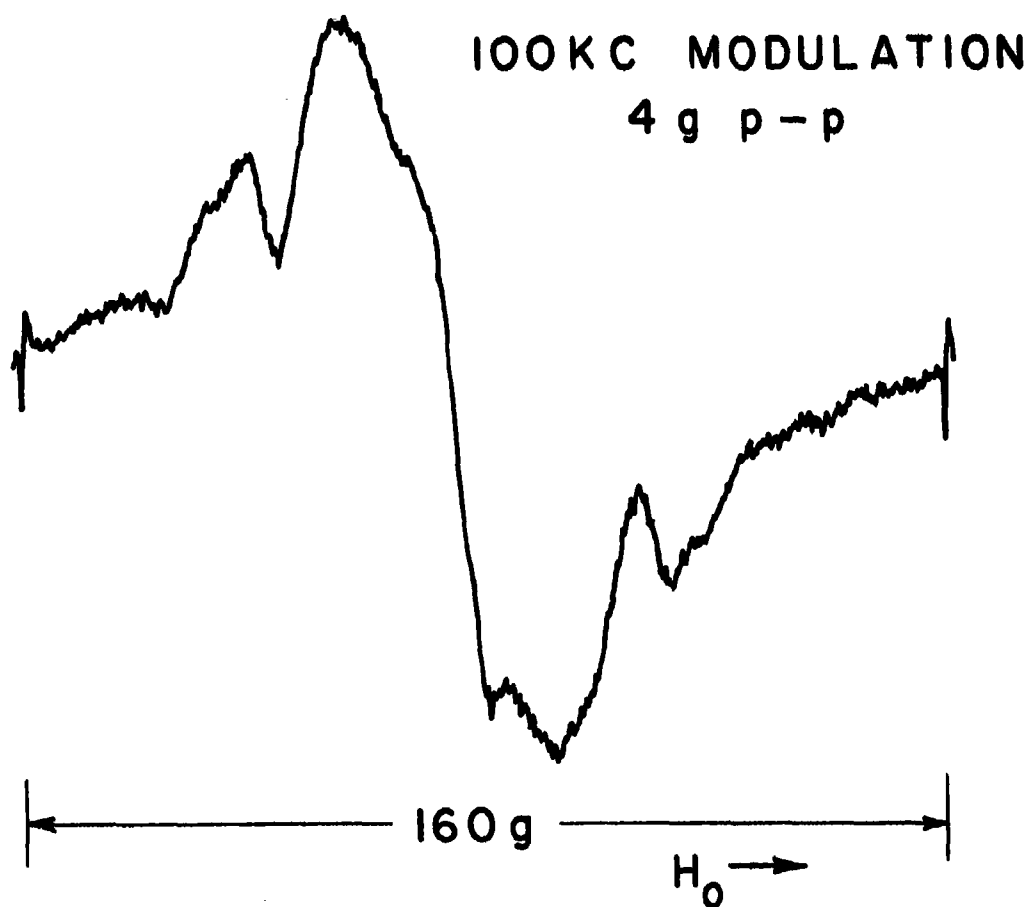


FIG. 31--First derivative trace of paramagnetic resonance absorption developed in bovine hemoglobin after ultraviolet irradiation at 77° K. Only the weak pre-irradiation absorption could be detected in this sample when it was warmed to room temperature. H_1 field was approximately 0.07 gauss.

production of thermoluminescence. The number of unpaired spins in ultraviolet irradiated amino acids is several orders of magnitude greater than the number of photons emitted during thermoluminescence.

SUMMARY

The research reported in this thesis has shown that certain amino acids, other closely related molecules, amino acid polymers and proteins develop metastable excited states with very long lifetimes (hours) when irradiated with ultraviolet light at 77° K. Transitions from these states to states of lower energy result in the emission of light. This light, in the form of thermoluminescence, has been observed upon heating the compounds following ultraviolet irradiation. The wavelength of exciting light is in the range $2400 \leq \lambda \leq 3900 \text{ \AA}$. The maximum of the observed thermoluminescence is in the region from 4000 to 4500 \AA . Experimental results are consistent with the hypothesis that the metastable excited state is molecular rather than crystalline in nature. (1) Thermoluminescence has been detected from compounds in aqueous solution and after freeze drying. (2) The luminescence intensity can be described in terms of monomolecular kinetics. (3) The wavelength of the absorbing light is in the region of an absorption band of the molecules involved. The metastable state involved is believed to arise in a charge trapping complex of the molecule and a metallic ion. A new expression for thermoluminescence intensity from polymers, based on a Markov process charge migration model, has been derived.

We have shown that ultraviolet irradiation of these compounds at 77° K also produces in many cases electron paramagnetic resonance absorption. The aromatic amino acids develop a single absorption line with a g -value close to that of DPPH. The intensity of absorption is greater in those molecules which contain hydroxy groups on the ring than in those which do not. Cysteine has been found to develop a hyperfine structure which

suggests that a dimer is formed. The EPR absorption spectra of several other amino acids and several proteins have been measured. In general the intensity of the absorption is much reduced after the samples are warmed to room temperature. It has not been possible however to show a correlation between the EPR absorption and thermoluminescence. The absorption is believed due to trapped free radical intermediates of photo-chemical reactions.

This research, particularly the thermoluminescence work, supports the belief that charge migration via some hopping mechanism may take place within protein molecules. This work shows that ultraviolet light may initiate the charge migration, and it suggests that metal ions play an important role in the charge migration and trapping processes.

APPENDIX I

The Born-Oppenheimer approximation can be used to derive what has been called $C(t)$, the probability per unit time that a charge will be thermally excited out of a trap. The trap is thought of as a positive atom or ion situated in a solid. The Hamiltonian for the electron-ion system can be written as

$$\mathcal{H} = \mathcal{H}_N + \mathcal{H}_e + V \quad (\text{A-1})$$

where \mathcal{H}_N is the kinetic and potential energy operator for the positive atom, \mathcal{H}_e represents the kinetic energy of the electron and its interaction with the rest of the solid or molecule, and V is the interaction of the electron with the positive atom. In the calculation, V rather than the interaction with the molecule or solid as a whole is assumed to determine the shape of the trapped electron-wave function.

The essence of the first-order Born-Oppenheimer approximation is the factorization of the eigenfunction of (A-1) into two functions in the following way. Considering the coordinates Q of the trapped atom and the rest of the solid as fixed, one finds the solution of the Schrödinger equation for the electron with coordinates q to be

$$[\mathcal{H}_e + V(q, Q)]\varphi_1(q, Q) = \epsilon_1(Q)\varphi_1(q, Q) . \quad (\text{A-2})$$

The eigenvalue $\epsilon_1(Q)$ which appears in this equation serves as the potential produced by the electron at the position of the positive atom in the Schrödinger equation for this atom, which is

$$[\mathcal{H}_N + \epsilon_1(Q)]x_{1\alpha}(Q) = E_{1\alpha}x_{1\alpha}(Q) . \quad (\text{A-3})$$

The factorization mentioned above consists of writing the eigenfunction of (A-1) as

$$\psi_{1\alpha}(q, Q) = \varphi_1(q, Q)x_{1\alpha}(Q) . \quad (\text{A-4})$$

Operating on (A-4) with (A-1), one obtains

$$\begin{aligned} \mathcal{H} \Psi_{i\alpha}(q, Q) &= [\mathcal{H}_N + \epsilon_i(Q)] \phi_i(q, Q) \chi_{i\alpha}(Q) \\ &= E_{i\alpha} \Psi_{i\alpha}(q, Q) + \mathcal{H}' \Psi_{i\alpha}(q, Q) \end{aligned} \quad (\text{A-5})$$

where

$$\mathcal{H}' \Psi_{i\alpha}(q, Q) = [\mathcal{H}_N \phi_i(q, Q)] \chi_{i\alpha}(Q) . \quad (\text{A-6})$$

The term $\mathcal{H}' \Psi_{i\alpha}$ is nonvanishing because the differential operators in \mathcal{H}_N act upon the atomic coordinates Q which appear as parameters in $\phi_i(q, Q)$.

The operator \mathcal{H}' is the perturbation which provides the electron-phonon interaction necessary for the thermal release of the trapped charge. Let i, α represent the quantum numbers of the trapped electron and positive atom, let j, β be the quantum numbers for the electron and atom after the electron has escaped. Then the transition or release rate $\omega(i\alpha \rightarrow j\beta)$ as given by ordinary time dependent perturbation theory is

$$\omega(i\alpha \rightarrow j\beta) = \frac{2\pi}{\hbar} \left| \int \Psi_{j\beta}^* \mathcal{H}' \Psi_{i\alpha} d^3q d^3Q \right|_{\rho_f}^2 \quad (\text{A-7})$$

where ρ_f is the density of final states and where the energy of the final state must equal that of the initial state.

The actual transition rate for the release of trapped electrons is the sum of $\omega(i\alpha \rightarrow j\beta)$ over all initial states weighted by the Boltzman factor and over all final states consistent with the requirement $E_{i\alpha} = E_{j\beta}$. Kubo has calculated this sum. To do so, he assumes that the motion of the positive atom is that of a three-dimensional harmonic oscillator with frequency ω if an electron is trapped, ω' if not. The initial electron state is hydrogenlike, the final state is represented by a plane wave. With these approximations, he finds that the actual transition

rate is

$$W = A \left(\frac{\delta}{2} \right)^{[(\epsilon/\hbar\omega)-1]} \exp\left(-\frac{\epsilon}{kT}\right) \quad \frac{\hbar\omega}{kT} \text{ large} \quad (\text{A-8})$$

$$A \left(\frac{kT}{\hbar\omega} \right) \exp\left[-\frac{\epsilon}{kT(2\delta - \delta^2)}\right] \quad \frac{\hbar\omega}{kT} \text{ small} \quad (\text{A-9})$$

In these formulae, ϵ is the energy difference between the trapped and free states of the electron, δ is defined by the relation $(\omega'/\omega) = 1 - \delta$, $A = 256(m/M)(\omega\omega')^{1/2}$, where m and M are the masses of the electron and atom, respectively.

APPENDIX II

The first program which appears below was employed in computing glow curves - Eq. (2-26) - for L-phenylalanine. These curves are shown in Fig. 20.

The second program was used in computing the glow curve, Eq. (2-65), for a four-unit polymer.

\$\$\$ TIME ON 1116

WEDNESDAY, 6/6/62

S538

JOB

6MIN GILL, JIM BIOPHYSICS CONTACT TESLER

BURROUGHS ALGEBRAIC COMPILER - STANFORD VERSION 7/25/61\$

INTEGER A,K\$

ARRAY II(5),

THETA(5) = (1.07**3, 1.27**3,

1.47**3, 1.27**3, 1.27**3), GAMMA (5) =(1.25**4,

7.57**4, 4.46**5, 1.25**4, 4.46**5)\$

WRITE (\$\$TIT,IES)\$

WRITE (\$\$ISS,UES)\$

LE=86\$ RI=4\$

FOR T = (0.02, 0.02, 0.54)\$

ENTER INTEG\$

LE=73.06\$ RI=27.97\$

FOR T = (0.56, 0.02, 2.0)\$

ENTER INTEG\$

LE=76\$ RI=26.5\$

FOR T = (2.02, 0.02, 3.0)\$

ENTER INTEG\$

```

LE=83.5$ RI=24$
FOR T = (3.02, 0.02, 4.0)$
  ENTER INTEG$
  WRITE($$COY)$
  GO FLUSHIT$
  SUBROUTINE INTEG$
    BEGIN
      TE=1/(LE+RI.T)$
      TEA=1/(LE+RI.(T-0.005))$
      TEB=1/(LE+RI.(T-0.01))$
      TEC=1/(LE+RI.(T-0.015))$
      TED=1/(LE+RI.(T-0.02))$
      FOR A = (1,1,5)$
        BEGIN
          THAT=-THETA(A)$
          TEETH=TEETH+(TEETH=EXP(TEC.THAT)+EXP(TEA.THAT))$
          BATH=EXP(TEB.THAT)$
          II(A)= II(A)+(1.6666666**-3)(TEETH+TEETH+BATH+BATH+EXP(TED.THAT)
                                +EXP(TE.THAT))$
        END$
      WRITE ($$VAL,UES)$
      RETURN
    END$
  OUTPUT VAL(T, FOR K=(1,1,5)$ GAMMA(K).EXP(-THETA(K).TE).EXP(-GAMMA(K)
                                .II(K))),
  ISS(T, FOR K=(1,1,5)$ GAMMA(K).EXP(-THETA(K)/86.0)),
  TIT(FOR K = (1,1,5)$ GAMMA(K), FOR K=(1,1,5)$ THETA(K))$

```

```

FORMAT UES(X4.2, B5, 3(B2, X18.8), W0),
LES(B2, *GAMMA = *, B1, 3(B6, F9.3, B5), W0, B2, *THETA = *,
      B1, 3(B6, F9.3, B5), W2, B1, *T=*, W0, B1, *--*, W2),
COY(B2, *NO MORE VALUES OF I(T) TO COMPUTE*, W0)$
FLUSHIT.. FINISH$

```

COMPILED PROGRAM ENDS AT 0552
PROGRAM VARIABLES BEGIN AT 9281

- - -

\$\$\$ TIME ON 1109

WEDNESDAY, 6/6/62

S538 JOB 7MIN GILL, JIM BIOPHYSICS CONTACT TESLER

BURROUGHS ALGEBRAIC COMPILER - STANFORD VERSION 7/25/61\$

GAMMA=7.57**4\$

THETA=1.27**3\$ II=0\$ THAT=1.27**3\$SQ=SQRT(2)\$ ST=SQRT(3)\$

SQA=(1+SQ)/4\$

SQB=(1-SQ)/4\$

SQC=(1/SQ-1)GAMMA\$

SQD=(-1/SQ-1)GAMMA\$

STA=(3+ST)/12\$

STB=(3-ST)/12\$

STC=(ST/2-1)GAMMA\$

STD=(-ST/2-1)GAMMA\$

WRITE(\$\$TIT, LES)\$

WRITE (\$\$ISS, UES)\$

```

LE=86$ RI=4$
FOR T = (0.02, 0.02, 0.54)$
  ENTER INTEG$
LE=73.06$ RI=27.97$
FOR T = (0.56, 0.02, 2.0)$
  ENTER INTEG$
LE=76$ RI = 26.5$
FOR T = (2.02, 0.02, 3.0)$
  ENTER INTEG$
LE=83.5$ RI=24$
FOR T = (3.02, 0.02, 4.0)$
  ENTER INTEG$
WRITE ($$COY)$
GO FLUSHIT$
SUBROUTINE INTEG$
  BEGIN
    TEETH=TEETH+(TEETH=EXP(THAT/(LE+RI.(T-0.015)))+EXP(THAT/(LE+RI
      .(T-0.005))))$
    BATH=EXP(THAT/(LE+RI.(T-0.01)))$
    II=II+(1.6666666**-3) (TEETH+TEETH+BATH+BATH+EXP(THAT/(LE+RI
      .(T-0.02)))+EXP(THAT/(LE+RI.T)))$
    WRITE($$VAL,UES)$
  RETURN
  END$
COMMENT THE 6 IN THE DENOMINATORS IS 1/N(O) $

```

```

OUTPUT VAL(T, (GAMMA.EXP(THAT/(LE+RI.T)))(EXP(-GAMMA.II)
+SQA.EXP(SQC.II)+SQB.EXP(SQD.II)+STA.EXP(STC.II)
+STB.EXP(STD.II))/6),
ISS(T, (GAMMA.EXP(THAT/86))(1+SQA+SQB+STA+STB)/6),
TIT(GAMMA, THETA)$
FORMAT UES(X4.2,B7,X18.8W),
LES (B2,*GAMMA = *,B7,F9.3,W,B2,*THETA = *,B7,F9.3,W2,
B1,*T=*,W,B1,*--*,W2),
COY(B2, *NO MORE VALUES OF I(T) TO COMPUTE*, WO)$
FLUSHIT.. FINISH$

```

```

COMPILED PROGRAM ENDS AT 0561
PROGRAM VARIABLES BEGIN AT 9225

```